

1 **We would like to thank the editor for the recommendations, which we think helped to improve the**
2 **quality and clarity of this manuscript. We hope our responses and adaptations are adequate to**
3 **accept this manuscript for publication in Biogeosciences. Please find our detailed responses below.**

4
5 **Associate Editor Comment (8. November 2017)**
6

7
8 Dear authors,
9

10 I checked your modifications and I am satisfied by your efforts of synthesis. I have some additional
11 recommendations:

12
13 - Your manuscript includes too many items (figures and tables). Please select six items that will be
14 presented in the main text and prepare supplementary files for the other items.

15
16 - Your discussion has too many subtitles. Could you simplify the structuration by, for example,
17 including some titles in the paragraph? To make it visible you can format it in bold or italic.

18
19 Thank you for having submitted to Biogeosciences this nice piece of work.
20

21 Sébastien
22
23

24 **Authors Reply:**

- 25 - **Even though we are aware that we have many figures, we do think that all of them are**
26 **necessary, which is why we would like to keep them in the manuscript instead of moving**
27 **some to the supplement.**
- 28
29 - **We deleted the subheadings (3-level) in the discussion part, as well as the 4-level**
30 **subheadings in the Material and Methods Part. Instead, we converted them into titles in**
31 **bold and italic to make the separation between paragraphs visible.**
- 32
33 - **We added one reference in the paper (introduction part, line 105)**
34
35

36

37

38

39

40

41 **Microbial methanogenesis in the sulfate-reducing zone of sediments in**
42 **the Eckernförde Bay, SW Baltic Sea**

43 Johanna Maltby^{a,b*}, Lea Steinle^{c,a}, Carolin R. Löscher^{d,a}, Hermann W. Bange^a, Martin A. Fischer^e, Mark
44 Schmidt^a, Tina Treude^{f,g*}

45 ^a *GEOMAR Helmholtz Centre for Ocean Research Kiel, Department of Marine Biogeochemistry, 24148*
46 *Kiel, Germany*

47 ^b *Present Address: Natural Sciences Department, Saint Joseph's College, Standish, Maine 04084, USA*

48 ^c *Department of Environmental Sciences, University of Basel, 4056 Basel, Switzerland*

49 ^d *Nordic Center for Earth Evolution, University of Southern Denmark, 5230 Odense, Denmark*

50 ^e *Institute of Microbiology, Christian-Albrecht-University Kiel, 24118 Kiel, Germany*

51 ^f *Department of Earth, Planetary, and Space Sciences, University of California Los Angeles (UCLA), Los*
52 *Angeles, California 90095-1567, USA*

53 ^g *Department of Atmospheric and Oceanic Sciences, University of California Los Angeles (UCLA), Los*
54 *Angeles, California 90095-1567, USA*

55
56 *Correspondence: jmaltby@sjcme.edu, ttreude@g.ucla.edu

57

58

59

60

61

62

63

64

65

66

67 **Abstract**

68 Benthic microbial methanogenesis is a known source of methane in marine systems. In most
69 sediments, the majority of methanogenesis is located below the sulfate-reducing zone, as sulfate
70 reducers outcompete methanogens for the major substrates hydrogen and acetate. Coexistence of
71 methanogenesis and sulfate reduction has been shown before and is possible by usage of non-
72 competitive substrates by the methanogens such as methanol or methylated amines. However, the
73 knowledge about magnitude, seasonality and environmental controls on this non-competitive
74 methane production is sparse. In the present study, the presence of methanogenesis within the
75 sulfate reduction zone (SRZ methanogenesis), was investigated in sediments (0-30 centimeters below
76 seafloor, cmbsf) of the seasonally hypoxic Eckernförde Bay, southwestern Baltic Sea. Water column
77 parameters such as oxygen, temperature, and salinity together with porewater geochemistry and
78 benthic methanogenesis rates were determined in the sampling area "Boknis Eck" quarterly from
79 March 2013 to September 2014, to investigate the effect of seasonal environmental changes on the
80 rate and distribution of SRZ methanogenesis, to estimate its potential contribution to benthic
81 methane emissions, and to identify potential methanogenic groups responsible for SRZ
82 methanogenesis. The metabolic pathway of methanogenesis in the presence or absence of sulfate
83 reducers and after the addition of a non-competitive substrate was studied in four experimental
84 setups: 1) unaltered sediment batch incubations (net methanogenesis), 2) ¹⁴C-bicarbonate labeling
85 experiments (hydrogenotrophic methanogenesis), 3) manipulated experiments with addition of
86 either molybdate (sulfate reducer inhibitor), 2-bromoethane-sulfonate (methanogen inhibitor), or
87 methanol (non-competitive substrate, potential methanogenesis), 4) addition of ¹³C-labeled
88 methanol (potential methylotrophic methanogenesis). After incubation with methanol, molecular
89 analyses were conducted to identify key functional methanogenic groups during methylotrophic
90 methanogenesis. To also compare magnitudes of SRZ methanogenesis with methanogenesis below
91 the sulfate reduction zone (> 30 cmbsf), hydrogenotrophic methanogenesis was determined by ¹⁴C-
92 bicarbonate radiotracer incubation in samples collected in September 2013.

93 SRZ methanogenesis changed seasonally in the upper 30 cmbsf with rates increasing from March (0.2
94 nmol cm⁻³ d⁻¹) to November (1.3 nmol cm⁻³ d⁻¹) 2013 and March (0.2 nmol cm⁻³ d⁻¹) to September (0.4
95 nmol cm⁻³ d⁻¹) 2014, respectively. Its magnitude and distribution appeared to be controlled by
96 organic matter availability, C/N, temperature, and oxygen in the water column, revealing higher rates
97 in warm, stratified, hypoxic seasons (September/November) compared to colder, oxygenated
98 seasons (March/June) of each year. The majority of SRZ methanogenesis was likely driven by the
99 usage of non-competitive substrates (e.g., methanol and methylated compounds), to avoid
100 competition with sulfate reducers, as it was indicated by the 1000-3000-fold increase in potential
101 methanogenesis activity observed after methanol addition. Accordingly, competitive

102 hydrogenotrophic methanogenesis increased in the sediment only below the depth of sulfate
103 penetration (> 30 cmbsf). Members of the family *Methanosarcinaceae*, which are known for
104 methylotrophic methanogenesis, were detected by PCR using *Methanosarcinaceae*-specific primers
105 and are likely to be responsible for the observed SRZ methanogenesis.
106 The present study indicates that SRZ methanogenesis is an important component of the benthic
107 methane budget and carbon cycling in Eckernförde Bay. Although its contribution to methane
108 emissions from the sediment into the water column are probably minor, SRZ methanogenesis could
109 directly feed into methane oxidation above the sulfate-methane transition zone.

110 1. Introduction

111 After water vapor and carbon dioxide, methane is the most abundant greenhouse gas in the
112 atmosphere (e.g. Hartmann et al., 2013; Denman et al., 2007). Its atmospheric concentration
113 increased more than 150 % since preindustrial times, mainly through increased human activities such
114 as fossil fuel usage and livestock breeding (Hartmann et al., 2013; Wuebbles & Hayhoe, 2002;
115 Denman et al., 2007). Determining the natural and anthropogenic sources of methane is one of the
116 major goals for oceanic, terrestrial and atmospheric scientists to be able to predict further impacts
117 on the world's climate. The ocean is considered to be a modest natural source for atmospheric
118 methane (Wuebbles & Hayhoe, 2002; Reeburgh, 2007; EPA, 2010). However, research is still sparse
119 on the origin of the observed oceanic methane, which automatically leads to uncertainties in current
120 ocean flux estimations (Bange et al., 1994; Naqvi et al., 2010; Bakker et al., 2014).

121 Within the marine environment, the coastal areas (including estuaries and shelf regions) are
122 considered the major source for atmospheric methane, contributing up to 75 % to the global ocean
123 methane production (Bange et al., 1994). The major part of the coastal methane is produced during
124 microbial methanogenesis in the sediment, with probably only a minor part originating from
125 methane production within the water column (Bakker et al., 2014). However, the knowledge on
126 magnitude, seasonality and environmental controls of benthic methanogenesis is still limited.

127 In marine sediments, methanogenesis activity is mostly restricted to the sediment layers below
128 sulfate reduction, due to the successful competition of sulfate reducers with methanogens for the
129 mutual substrates acetate and hydrogen (H₂) (Oremland & Polcin, 1982; Crill & Martens, 1986;
130 Jørgensen, 2006). Methanogens produce methane mainly from using acetate (acetoclastic
131 methanogenesis) or H₂ and carbon dioxide (CO₂) (hydrogenotrophic methanogenesis). Competition
132 with sulfate reducers can be relieved through usage of non-competitive substrates (e.g. methanol or
133 methylated compounds, methylotrophic methanogenesis) (Cicerone & Oremland, 1988; Oremland &
134 Polcin, 1982). Coexistence of sulfate reduction and methanogenesis has been detected in a few
135 studies from organic-rich sediments, e.g., salt-marsh sediments (Oremland et al., 1982; Buckley et al.,

136 2008), coastal sediments (Holmer & Kristensen, 1994; Jørgensen & Parkes, 2010) or sediments in
137 upwelling regions (Pimenov et al., 1993; Ferdelman et al., 1997; Maltby et al., 2016), indicating the
138 importance of these environments for methanogenesis within the sulfate reduction zone (SRZ
139 methanogenesis). So far, however, environmental controls of SRZ methanogenesis remain elusive.
140 The coastal inlet Eckernförde Bay (southwestern Baltic Sea) is an excellent model environment to
141 study seasonal and environmental controls of benthic SRZ methanogenesis. Here, the muddy
142 sediments are characterized by high organic loading and high sedimentation rates (Whiticar, 2002),
143 which lead to anoxic conditions within the uppermost 0.1-0.2 centimeter below seafloor (cmbsf)
144 (Preisler et al., 2007). Seasonally hypoxic (dissolved oxygen < 63 μM) and anoxic (dissolved oxygen =
145 0 μM) events in the bottom water of Eckernförde Bay (Lennartz et al., 2014; Steinle et al., 2017)
146 provide ideal conditions for anaerobic processes at the sediment surface.

147 Sulfate reduction is the dominant pathway of organic carbon degradation in Eckernförde Bay
148 sediments in the upper 30 cmbsf, followed by methanogenesis in deeper sediment layers where
149 sulfate is depleted (>> 30 cmbsf) (Whiticar 2002; Treude et al. 2005; Martens et al. 1998) (Fig. 1). This
150 methanogenesis below the sulfate-methane transition zone (SMTZ) can be intense and often leads to
151 methane oversaturation in the porewater below 50 cm sediment depth, resulting in gas bubble
152 formation (Abegg & Anderson, 1997; Whiticar, 2002; Thießén et al., 2006). Thus, methane is
153 transported from the methanogenic zone (> 30 cmbsf) to the surface sediment by both molecular
154 diffusion and advection via rising gas bubbles (Wever et al., 1998; Treude et al., 2005a). Although
155 upward diffusing methane is mostly retained by anaerobic oxidation of methane (AOM) (Treude et
156 al. 2005), a major part is reaching the sediment-water interface through gas bubble transport
157 (Treude et al. 2005; Jackson et al. 1998), resulting in a supersaturation of the water column with
158 respect to atmospheric methane concentrations (Bange et al., 2010). The Time Series Station “Boknis
159 Eck” in the Eckernförde Bay is a known site of methane emissions into the atmosphere throughout
160 the year due to this supersaturation of the water column (Bange et al., 2010).

161 The source for benthic and water column methane was seen in methanogenesis below the SMTZ (>>
162 30 cmbsf) (Whiticar, 2002), however, coexistence of sulfate reduction and methanogenesis has been
163 postulated (Whiticar, 2002; Treude et al., 2005a). Still, the magnitude and environmental controls of
164 SRZ methanogenesis is poorly understood, even though it may make a measurable contribution to
165 benthic methane emissions given its short diffusion distance to the sediment-water interface (Knittel
166 & Boetius, 2009). Production of methane within the sulfate reduction zone of Eckernförde Bay
167 sediments could further explain peaks of methane oxidation observed in top sediment layers, which
168 was previously attributed to methane transported to the sediment surface via rising gas bubbles
169 (Treude et al., 2005a).

170 In the present study, we investigated sediments from within (< 30 cmbsf, on a seasonal basis) and
171 below the sulfate reduction zone (> 30 cmbsf, on one occasion), and the water column (on a
172 seasonal basis) at the Time Series Station "Boknis Eck" in Eckernförde Bay, to validate the existence
173 of SRZ methanogenesis and its potential contribution to benthic methane emissions. Water column
174 parameters like oxygen, temperature, and salinity together with porewater geochemistry and
175 benthic methanogenesis were measured over a course of 2 years. In addition to seasonal rate
176 measurements, inhibition and stimulation experiments, stable isotope probing, and molecular
177 analysis were carried out to find out if SRZ methanogenesis 1) is controlled by environmental
178 parameters, 2) shows seasonal variability, 3) is based on non-competitive substrates with a special
179 focus on methylotrophic methanogens.

180 2. Material and Methods

181 2.1 Study site

182 Samples were taken at the Time Series Station "Boknis Eck" (BE, 54°31.15 N, 10°02.18 E;
183 www.bokniseck.de) located at the entrance of Eckernförde Bay in the southwestern Baltic Sea with a
184 water depth of about 28 m (map of sampling site can be found in e.g. Hansen et al., (1999)). From
185 mid of March until mid of September the water column is strongly stratified due to the inflow of
186 saltier North Sea water and a warmer and fresher surface water (Bange et al., 2011). Organic matter
187 degradation in the deep layers causes pronounced hypoxia (March-Sept) or even anoxia
188 (August/September) (Smetacek, 1985; Smetacek et al., 1984). The source of organic material is
189 phytoplankton blooms that occur regularly in spring (February-March) and fall (September-
190 November) and are followed by pronounced sedimentation of organic matter (Bange et al., 2011). To
191 a lesser extent, phytoplankton blooms and sedimentation are also observed during the summer
192 months (July/August) (Smetacek et al., 1984). Sediments at BE are generally classified as soft, fine-
193 grained muds (< 40 µm) with a carbon content of 3 to 5 wt% (Balzer et al., 1986). The bulk of organic
194 matter in Eckernförde Bay sediments originates from marine plankton and macroalgal sources (Orsi
195 et al., 1996), and its degradation leads to production of free methane gas (Wever & Fiedler, 1995;
196 Abegg & Anderson, 1997; Wever et al., 1998). The oxygen penetration depth is limited to the upper
197 few millimeters when bottom waters are oxic (Preisler et al., 2007). Reducing conditions within the
198 sulfate reduction zone lead to a dark grey/black sediments color with a strong hydrogen sulfur odor
199 in the upper meter of the sediment and dark olive-green color the deeper sediment layers (> 1 m)
200 (Abegg & Anderson, 1997).

201 **2.2 Water column and sediment sampling**

202 Sampling was done on a seasonal basis during the years of 2013 and 2014. One-Day field trips with
203 either F.S. Alkor (cruise no. AL410), F.K. Littorina or F.B. Polarfuchs were conducted in March, June,
204 and September of each year. In 2013, additional sampling was conducted in November. At each
205 sampling month, water profiles of temperature, salinity, and oxygen concentration (optical sensor,
206 RINKO III, detection limit= 2 μM) were measured with a CTD (Hydro-Bios). In addition, water samples
207 for methane concentration measurements were taken at 25 m water depth with a 6-Niskin bottle (4
208 Liter each) rosette attached to the CTD (Table 1). Complementary samples for water column
209 chlorophyll were taken at 25 m water depth with the CTD-rosette within the same months during
210 standardized monthly sampling cruises to Boknis Eck organized by GEOMAR.

211 Sediment cores were taken with a miniature multicorer (MUC, K.U.M. Kiel), holding 4 core liners
212 (length= 60 cm, diameter= 10 cm) at once. The cores had an average length of \sim 30 cm and were
213 stored at 10°C in a cold room (GEOMAR) until further processing (normally within 1-3 days after
214 sampling).

215 In September 2013, a gravity core was taken in addition to the MUC cores. The gravity core was
216 equipped with an inner plastic bag (polyethylene; diameter: 13 cm). After core recovery (330 cm
217 total length), the polyethylene bag was cut open at 12 different sampling depths resulting in intervals
218 of 30 cm and sampled directly on board for sediment porewater geochemistry (see Sect. 2.4),
219 sediment methane (see Sect. 2.5), sediment solid phase geochemistry (see Sect. 2.6), and microbial
220 rate measurements for hydrogenotrophic methanogenesis as described in section 2.8.

221 **2.3 Water column parameters**

222 At each sampling month, water samples for methane concentration measurements were taken at 25
223 m water depth in triplicates. Therefore, three 25 ml glass vials were filled bubble free directly after
224 CTD-rosette recovery and closed with butyl rubber stoppers. Biological activity in samples was
225 stopped by adding saturated mercury chloride solution, followed by storage at room temperature
226 until further treatment.

227 Concentrations of dissolved methane (CH_4) were determined by headspace gas chromatography as
228 described in Bange et al. (2010). Calibration for CH_4 was done by a two-point calibration with known
229 methane concentrations before the measurement of headspace gas samples, resulting in an error of
230 $< 5\%$.

231 Water samples for chlorophyll concentration were taken by transferring the complete water volume
232 (from 25 m water depth) from one water sampler into a 4.5 L Nalgene bottle, from which then
233 approximately 0.7-1 L (depending on the plankton content) were filtrated back in the GEOMAR
234 laboratory using GF/F filter (Whatman, 25 mm diameter, 8 μM pores size). Dissolved chlorophyll a

235 concentrations were determined using the fluorometric method by Welschmeyer (1994) with an
236 error < 10 %.

237 **2.4 Sediment porewater geochemistry**

238 Porewater was extracted from sediment within 24 hours after core retrieval using nitrogen (N₂) pre-
239 flushed rhizons (0.2 µm, Rhizosphere Research Products, Seeberg-Elverfeldt et al., 2005). In MUC
240 cores, rhizons were inserted into the sediment in 2 cm intervals through pre-drilled holes in the core
241 liner. In the gravity core, rhizons were inserted into the sediment in 30 cm intervals directly after
242 retrieval.

243 Extracted porewater from MUC and gravity cores was immediately analyzed for sulfide using
244 standardized photometric methods (Grasshoff et al., 1999).

245 Sulfate concentrations were determined using ion chromatography (Methrom 761). Analytical
246 precision was < 1 % based on repeated analysis of IAPSO seawater standards (dilution series) with an
247 absolute detection limit of 1 µM corresponding to a detection limit of 30 µM for the undiluted
248 sample.

249 For analysis of dissolved inorganic carbon (DIC), 1.8 ml of porewater was transferred into a 2 ml glass
250 vial, fixed with 10 µl saturated HgCl₂ solution and crimp sealed. DIC concentration was determined
251 as CO₂ with a multi N/C 2100 analyzer (Analytik Jena) following the manufacturer's instructions.
252 Therefore, the sample was acidified with phosphoric acid and the outgassing CO₂ was measured. The
253 detection limit was 20 µM with a precision of 2-3 %.

254 **2.5 Sediment methane concentrations**

255 In March 2013, June 2013 and March 2014, one MUC core was sliced in 1 cm intervals until 6 cmbsf,
256 followed by 2 cm intervals until the end of the core. At the other sampling months, the MUC core
257 was sliced in 1 cm intervals until 6 cmbsf, followed by 2 cm intervals until 10 cmbsf and 5 cm intervals
258 until the end of the core.

259 Per sediment depth (in MUC and gravity cores), 2 cm⁻³ of sediment were transferred into a 10 ml-
260 glass vial containing 5 ml NaOH (2.5 %) for determination of sediment methane concentration per
261 volume of sediment. The vial was quickly closed with a butyl septum, crimp-sealed and shaken
262 thoroughly. The vials were stored upside down at room temperature until measurement via gas
263 chromatography. Therefore, 100 µl of headspace was removed from the gas vials and injected into a
264 Shimadzu gas chromatograph (GC-2014) equipped with a packed Haysep-D column and a flame
265 ionization detector. The column temperature was 80°C and the helium flow was set to 12 ml min⁻¹.
266 CH₄ concentrations were calibrated against CH₄ standards (Scotty gases). The detection limit was 0.1
267 ppm with a precision of 2 %.

268 **2.6 Sediment solid phase geochemistry**

269 Following the sampling for CH₄, the same cores described under section 2.5 were used for the
270 determination of the sediment solid phase geochemistry, i.e. porosity, particulate organic carbon
271 (POC) and particulate organic nitrogen (PON).

272 Sediment porosity of each sampled sediment section was determined by the weight difference of 5
273 cm³ wet sediment after freeze-drying for 24 hours. Dried sediment samples were then used for
274 analysis of particulate organic carbon (POC) and particulate organic nitrogen (PON) with a Carlo-Erba
275 element analyzer (NA 1500). The detection limit for C and N analysis was < 0.1 dry weight percent (%)
276 with a precision of < 2 %.

277 **2.7 Sediment methanogenesis**

278 **2.7.1 Methanogenesis in MUC cores**

279 At each sampling month, three MUC cores were sliced in 1 cm intervals until 6 cmbsf, in 2 cm
280 intervals until 10 cmbsf, and in 5 cm intervals until the bottom of the core. Every sediment layer was
281 transferred to a separate beaker and quickly homogenized before sub-sampling. The exposure time
282 with air, i.e. oxygen, was kept to a minimum. Sediment layers were then sampled for determination
283 of net methanogenesis (defined as the sum of total methane production and consumption, including
284 all available methanogenic substrates in the sediment), hydrogenotrophic methanogenesis
285 (methanogenesis based on the substrates CO₂/H₂), and potential methanogenesis (methanogenesis
286 at ideal conditions, i.e. no lack of nutrients) as described in the following sections.

287 **2.7.1.1 Net methanogenesis**

288 Net methanogenesis was determined with sediment slurry experiments by measuring the headspace
289 methane concentration over time. Per sediment layer, triplicates of 5 cm³ of sediment were
290 transferred into N₂-flushed sterile glass vials (30 ml) and mixed with 5 ml filtered bottom water. The
291 slurry was repeatedly flushed with N₂ to remove residual methane and to ensure complete anoxia.
292 Slurries were incubated in the dark at in-situ temperature, which varied at each sampling date (Table
293 1). Headspace samples (0.1 ml) were taken out every 3-4 days over a time period of 4 weeks and
294 analyzed on a Shimadzu GC-2104 gas chromatograph (see Sect. 2.5). Net methanogenesis rates were
295 determined by the linear increase of the methane concentration over time (minimum of 6 time
296 points, see also Fig. S1).

297 **2.7.1.2 Hydrogenotrophic methanogenesis**

298 To determine if hydrogenotrophic methanogenesis, i.e., methanogenesis based on the competitive
299 substrates H₂, is present in the sulfate-reducing zone, radioactive sodium bicarbonate (NaH¹⁴CO₃)
300 was added to the sediment.

Formatted: Font: Calibri Light, Bold

Formatted: Font: Bold

301 Per sediment layer, sediment was sampled in triplicates with glass tubes (5 mL) which were closed
302 with butyl rubber stoppers on both ends according to (Treude et al. 2005). Through the stopper,
303 $\text{NaH}^{14}\text{CO}_3$ (dissolved in water, injection volume 6 μl , activity 222 kBq, specific activity = 1.85-2.22
304 GBq/mmol) was injected into each sample and incubated for three days in the dark at in-situ
305 temperature (Table 1). To stop bacterial activity, sediment was transferred into 50 ml glass-vials filled
306 with 20 ml sodium hydroxide (2.5 % w/w), closed quickly with rubber stoppers and shaken
307 thoroughly. Five controls were produced from various sediment depths by injecting the radiotracer
308 directly into the NaOH with sediment.
309 The production of ^{14}C -methane was determined with the slightly modified method by Treude et al.,
310 (2005) used for the determination of anaerobic oxidation of methane. The method was identical,
311 except no unlabeled methane was determined by gas chromatography. Instead, DIC values were
312 used to calculate hydrogenotrophic methane production.

313 **2.7.1.3 Potential methanogenesis in manipulated experiments**

314 To examine the interaction between sulfate reduction and methanogenesis, inhibition and
315 stimulation experiments were carried out. Therefore, every other sediment layer was sampled
316 resulting in the following examined six sediment layers: 0-1 cm, 2-3 cm, 4-5 cm, 6-8 cm, 10-15 cm
317 and 20-25 cm. From each layer, sediment slurries were prepared by mixing 5 ml sediment in a 1:1
318 ratio with adapted artificial seawater medium (salinity 24, Widdel & Bak, 1992) in N_2 -flushed, sterile
319 glass vials before further manipulations.

320 In total, four different treatments, each in triplicates, were prepared per depth: 1) with sulfate
321 addition (17 mM), 2) with sulfate (17 mM) and molybdate (22 mM) addition, 3) with sulfate (17 mM)
322 and 2-bromoethane-sulfonate (BES, 60 mM) addition, and 4) with sulfate (17 mM) and methanol (10
323 mM) addition. From here on, the following names are used to describe the different treatments,
324 respectively: 1) control treatment, 2) molybdate treatment, 3) BES treatment, and 4) methanol
325 treatment. Control treatments feature the natural sulfate concentrations occurring in sediments of
326 the sulfate reduction zone at the sampling site. Molybdate was used as an enzymatic inhibitor for
327 sulfate reduction (Oremland & Capone, 1988) and BES was used as an inhibitor for methanogenic
328 archaea (Hoehler et al., 1994). Methanol is a known non-competitive substrate, which is used by
329 methanogens but not by sulfate reducers (Oremland & Polcin, 1982), thus it is suitable to examine
330 non-competitive methanogenesis. Treatments were incubated similar to net methanogenesis
331 (2.7.1.1) by incubating sediment slurries at the respective in-situ temperature (Table 1) in the dark
332 for a time period of 4 weeks. Headspace samples (0.1 ml) were taken every 3-5 days over a time
333 period of 4 weeks and potential methanogenesis rates were determined by the linear increase of
334 methane concentration over time (minimum of 6 time points).

Formatted: Font: Calibri Light, Bold

335

336 **2.7.1.4 Potential methylophilic methanogenesis from methanol using stable isotope probing**

Formatted: Font: Calibri Light, Bold

337 One additional experiment was conducted with sediments from September 2014 by adding ¹³C-
338 labelled methanol to investigate the production of ¹³C-labelled methane. Three cores were stored at
339 1°C after the September 2014 cruise until further processing ~ 3.5 months later. The low storage
340 temperature together with the expected oxygen depletion in the enclosed supernatant water after
341 retrieval of the cores likely led to slowed anaerobic microbial activity during storage time and
342 preserved the sediments for potential methanogenesis measurements.

343 Sediment cores were sliced in 2 cm intervals and the upper 0-2 cmbsf sediment layer of all three
344 cores was combined in a beaker and homogenized. Then, sediment slurries were prepared by mixing
345 5 cm³ of sediment with 5 ml of artificial seawater medium in N₂-flushed, sterile glass vials (30 ml).
346 After this, methanol was added to the slurry with a final concentration of 10 mM (see 2.7.1.3).
347 Methanol was enriched with ¹³C-labelled methanol in a ratio of 1:1000 between ¹³C-labelled (99.9 %
348 ¹³C) and non-labelled methanol mostly consisting of ¹²C (manufacturer: Roth). In total, 54 vials were
349 prepared for nine different sampling time points during a total incubation time of 37 days. All vials
350 were incubated at 13°C (in situ temperature in September 2014) in the dark. At each sampling point,
351 six vials were stopped: one set of triplicates were used for headspace methane and carbon dioxide
352 determination and a second set of triplicates were used for porewater analysis.

353 Headspace methane and carbon dioxide concentrations (volume 100 µl) were determined on a
354 Shimadzu gas chromatograph (GC-2014) equipped with a packed Haysep-D column a flame ionization
355 detector and a methanizer. The methanizer (reduced nickel) reduces carbon dioxide with hydrogen
356 to methane at a temperature of 400°C. The column temperature was 80°C and the helium flow was
357 set to 12 ml min⁻¹. Methane concentrations (including reduced CO₂) were calibrated against methane
358 standards (Scotty gases). The detection limit was 0.1 ppm with a precision of 2 %.

359 Analyses of ¹³C/¹²C-ratios of methane and carbon dioxide were conducted after headspace
360 concentration measurements by using a continuous flow combustion gas chromatograph (Trace
361 Ultra, Thermo Scientific), which was coupled to an isotope ratio mass spectrometer (MAT253,
362 Thermo Scientific). The isotope ratios of methane and carbon dioxide given in the common delta-
363 notation (δ ¹³C in permill) are reported relative to Vienna Pee Dee Belemnite (VPDB) standard.
364 Isotope precision was +/- 0.5 ‰, when measuring near the detection limit of 10 ppm.

365 For porewater analysis of methanol concentration and isotope composition, each sediment slurry of
366 the triplicates was transferred into argon-flushed 15 ml centrifuge tubes and centrifuged for 6
367 minutes at 4500 rpm. Then 1 ml filtered (0.2 µm) porewater was transferred into N₂-flushed 2 ml
368 glass vials for methanol analysis, crimp sealed and immediately frozen at -20 °C. Methanol

369 concentrations and isotope composition were determined via high performance liquid
370 chromatography-ion ratio mass spectrometry (HPLC-IRMS, Thermo Fisher Scientific) at the MPI
371 Marburg. The detection limit was 50 μM with a precision of 0.3‰.

372 2.7.2 Methanogenesis in the gravity core

373 Ex situ hydrogenotrophic methanogenesis was determined in a gravity core taken in September 2013.
374 The pathway is thought to be the main methanogenic pathway in the sediment below the SMTZ in
375 Eckernförde Bay (Whiticar, 2002). Hydrogenotrophic methanogenesis was determined using
376 radioactive sodium bicarbonate ($\text{NaH}^{14}\text{CO}_3$). At every sampled sediment depth (12 depths in 30 cm
377 intervals), triplicate glass tubes (5 mL) were inserted directly into the sediment. Tubes were filled
378 bubble-free with sediment and closed with butyl rubber stoppers on both ends according to (Treude
379 et al. 2005). Methods following sampling were identical as described in 2.7.1.2.

380 2.8 Molecular analysis

381 During the non-labeled methanol treatment of the 0-1 cmbsf horizon from the September 2014
382 sampling (see 2.7.1.3), additional samples were prepared to detect and quantify the presence of
383 methanogens in the sediment. Therefore, additional 15 vials were prepared with addition of
384 methanol as described in 2.7.1.3 for five different time points (day 1 (= t_0), day 8, day 16, day 22, and
385 day 36) and stopped at each time point by transferring sediment from the triplicate slurries into
386 whirl-packs (Nasco), which then were immediately frozen at -20°C . DNA was extracted from ~ 500 mg
387 of sediment using the FastDNA[®] SPIN Kit for Soil (Biomedical). Quantitative real-time polymerase
388 chain reaction (qPCR) technique using TaqMan probes and TaqMan chemistry (Life Technologies) was
389 used for the detection of methanogens on a ViiA7 qPCR machine (Life Technologies). Primer and
390 Probe sets as originally published by Yu et al. (2005) were applied to quantify the orders
391 *Methanobacteriales*, *Methanosarcinales* and *Methanomicrobiales* along with the two families
392 *Methanosarcinaceae* and *Methanosetaeaceae* within the order *Methanosarcinales*. In addition, a
393 universal primer set for detection of the domain *Archaea* was used (Yu et al. 2005).
394 Absolute quantification of the 16S rDNA from the groups mentioned above was performed with
395 standard dilution series. The standard concentration reached from 10^8 to 10^1 copies per μL .
396 Quantification of the standards and samples was performed in duplicates. Reaction was performed in
397 a final volume of 12.5 μL containing 0.5 μL of each Primer ($10\text{pmol } \mu\text{L}^{-1}$, MWG), 0.25 μL of the
398 respective probe ($10\text{ pmol } \mu\text{L}^{-1}$, Life Technologies), 4 μL H_2O (Roth), 6.25 μL TaqMan Universal Master
399 Mix II (Life Technologies) and 1 μL of sample or standard. Cycling conditions started with initial
400 denaturation and activation step for 10 min at 95°C , followed by 45 cycles of 95°C for 15 sec, 56°C
401 for 30 sec and 60°C for 60 sec. Non-template controls were run in duplicates with water instead of
402 DNA for all primer and probe sets, and remained without any detectable signal after 45 cycles.

403 2.9 Statistical Analysis

404 To determine possible environmental control parameters of SRZ methanogenesis, a Principle
405 Component Analysis (PCA) was applied according to the approach described in Gier et al. (2016).
406 Prior to PCA, the dataset was transformed into ranks to assure the same data dimension.
407 In total, two PCAs were conducted. The first PCA was used to test the relation of parameters in the
408 surface sediment (integrated methanogenesis (0-5 cm, $\text{mmol m}^{-2} \text{d}^{-1}$), POC content (average value
409 from 0-5 cmbsf, wt %), C/N (average value from 0-5 cmbsf, molar) and the bottom water (25 m water
410 depth) (oxygen (μM), temperature ($^{\circ}\text{C}$), salinity (PSU), chlorophyll ($\mu\text{g L}^{-1}$), methane (nM)). The
411 second PCA was applied on depth profiles of sediment SRZ methanogenesis ($\text{nmol cm}^{-3} \text{d}^{-1}$), sediment
412 depth (cm), sediment POC content (wt%), sediment C/N ratio (molar), and sampling month (one
413 value per depth profile at a specific month, the later in the year the higher the value).
414 For each PCA, biplots were produced to view data from different angles and to graphically determine
415 a potential positive, negative or zero correlation between methanogenesis rates and the tested
416 variables.

417 3. Results

418 3.1 Water column parameters

419 From March 2013 to September 2014, the water column had a pronounced temporal and spatial
420 variability of temperature, salinity, and oxygen (Fig. 2 and 3). In 2013, temperature of the upper
421 water column increased from March (1°C) to September (16°C), but decreased again in November
422 (11°C). The temperature of the lower water column increased from March 2013 (2°C) to November
423 2013 (12°C). In 2014, lowest temperatures of the upper and lower water column were reached in
424 March (4°C). Warmer temperatures of the upper water column were observed in June and
425 September (around 17°C), while the lower water column peaked in September (13°C).
426 Salinity increased over time during 2013, showing the highest salinity of the upper and lower water
427 column in November (18 and 23 PSU, respectively). In 2014, salinity of the upper water column was
428 highest in March and September (both 17 PSU), and lowest in June (13 PSU). The salinity of the lower
429 water column increased from March 2014 (21 PSU) to September 2014 (25 PSU).
430 In both years, June and September showed the most pronounced vertical gradient of temperature
431 and salinity, featuring a pycnocline at around ~ 14 m water depth.
432 Summer stratification was also seen in the O_2 profiles, which showed O_2 depleted conditions ($\text{O}_2 <$
433 $150 \mu\text{M}$) in the lower water column from June to September in both years, reaching concentrations
434 below 1- 2 μM (detection limit of CTD sensor) in September of both years (Fig. 2 and 3). The water
435 column was completely ventilated, i.e. homogenized, in March of both years with O_2 concentrations
436 of 300-400 μM down to the sea floor at about 28 m.

437

438 3.2 Sediment geochemistry in MUC cores

439 Sediment porewater and solid phase geochemistry results for the years 2013 and 2014 are shown in
440 Fig. 2 and 3, respectively.

441 Sulfate concentrations at the sediment surface ranged between 15-20 mM. Concentration decreased
442 with depth at all sampling months but was never fully depleted until the bottom of the core (18-29
443 cmbsf, between 2 and 7 mM sulfate). November 2013 showed the strongest decrease from ~20 mM
444 at the top to ~2 mM at the bottom of the core (27 cmbsf).

445 Opposite to sulfate, methane concentration increased with sediment depth in all sampling months
446 (Fig. 2 and 3). Over the course of a year (i.e. March to November in 2013, and March to September in
447 2014), maximum methane concentration increased, reaching the highest concentration in November
448 2013 (~1 mM at 26 cmbsf) and September 2014 (0.2 mM at 23 cmbsf), respectively. Simultaneously,
449 methane profiles became steeper, revealing higher methane concentrations at shallower sediment
450 depth late in the year. Magnitudes of methane concentrations were similar in the respective months
451 of 2013 and 2014.

452 In all sampling months, sulfide concentration increased with sediment depth (Fig. 2 and 3). Similar to
453 methane, sulfide profiles revealed higher sulfide concentrations at shallower sediment depth
454 together with higher peak concentrations over the course the sampled months in each sampling
455 year. Accordingly, November 2013 (10.5 mM at 15 cmbsf) and September 2014 (2.8 mM at 15
456 cmbsf) revealed the highest sulfide concentrations, respectively. September 2014 was the only
457 sampling month showing a pronounced decrease in sulfide concentration from 15 cmbsf to 21 cmbsf
458 of over 50 %.

459 DIC concentrations increased with increasing sediment depth at all sampling months. Concomitant
460 with highest sulfide concentrations, highest DIC concentration was detected in November 2013 (26
461 mM at 27 cmbsf). At the surface, DIC concentrations ranged between 2-3 mM at all sampling
462 months. In June of both years, DIC concentrations were lowest at the deepest sampled depth
463 compared to the other sampling months (16 mM in 2013, 13 mM in 2014).

464 At all sampling months, POC profiles scattered around 5 ± 0.9 wt % with depth. Only in November
465 2013, June 2014 and September 2014, POC content exceeded 5 wt % in the upper 0-1 cmbsf (5.9, 5.2
466 and 5.3 wt %, respectively) with the highest POC content in November 2013. Also in November 2013,
467 surface C/N ratio (0-1 cmbsf) of the particulate organic matter was lowest of all sampling months
468 (8.6). In general, C/N ratio increased with depth in both years with values around 9 at the surface and
469 values around 10-11 at the deepest sampled sediment depths.

470 **3.3 Sediment geochemistry in gravity cores**

471 Results from sediment porewater and solid phase geochemistry in the gravity core from September
472 2013 are shown in Fig. 4. Please note that the sediment depth of the gravity core was corrected by
473 comparing the sulfate concentrations at 0 cmbsf in the gravity core with the corresponding sulfate
474 concentration and depth in the MUC core from September 2013 (Fig. 2). The soft surface sediment is
475 often lost during the gravity coring procedure. Through this correction, the topmost layer of the
476 gravity core was set at a depth of 14 cmbsf.

477 Porewater sulfate concentration in the gravity core decreased with depth (i.e. below 0.1 mM at 107
478 cmbsf) and stayed below 0.1 mM until 324 cmbsf. Sulfate increased slightly (1.9 mM) at the bottom
479 of the core (345 cmbsf). In concert with sulfate, also methane, sulfide, DIC, POC and C/N profiles
480 showed distinct alteration in the profile at 345 cmbsf (see below, Fig. 4). As fluid seepage has not
481 been observed at the Boknis Eck station (Schlüter et al., 2000), these alterations could either indicate
482 a change in sediment properties or result from a sampling artifact from the penetration of seawater
483 through the core catcher into the deepest sediment layer. The latter process is, however, not
484 expected to considerably affect sediment solid phase properties (POC and C/N), and we therefore
485 dismissed this hypothesis.

486 Methane concentration increased steeply with depth reaching a maximum of 4.8 mM at 76 cmbsf.
487 Concentration stayed around 4.7 mM until 262 cmbsf, followed by a slight decrease until 324 cmbsf
488 (2.8 mM). From 324 cmbsf to 345 cmbsf methane increased again (3.4 mM).

489 Both sulfide and DIC concentrations increased with depth, showing a maximum at 45 cmbsf (~5mM)
490 and 345 cmbsf (~1mM), respectively. While sulfide decreased after 45 cmbsf to a minimum of ~300
491 μM at 324 cmbsf, it slightly increased again to ~1 mM at 345 cmbsf. In accordance, DIC
492 concentrations showed a distinct decrease between 324 cmbsf to 345 cmbsf (from 45 mM to 39
493 mM).

494 While POC contents varied around 5 wt % throughout the core, C/N ratio slightly increased with
495 depth, revealing the lowest ratio at the surface (~3) and the highest ratio at the bottom of the core
496 (~13). However, both POC and C/N showed a distinct increase from 324 cmbsf to 345 cmbsf.

497

498 **3.4 Methanogenesis activity in MUC cores**

499 **3.4.1 Net methanogenesis**

500 Net methanogenesis activity (calculated by the linear increase of methane over time, see Fig. S1) was
501 detected throughout the cores at all sampling months (Fig. 2 and 3). Activity measured in MUC cores
502 increased over the course of the year in 2013 and 2014 (that is: March to November in 2013 and
503 March to September in 2014) with lower rates mostly $< 0.1 \text{ nmol cm}^{-3} \text{ d}^{-1}$ in March and higher rates $>$

504 0.2 nmol cm⁻³ d⁻¹ in November 2013 and September 2014, respectively. In general, November 2013
505 revealed highest net methanogenesis rates (1.3 nmol cm⁻³ d⁻¹ at 1-2 cmbsf). Peak rates were
506 detected at the sediment surface (0-1 cmbsf) at all sampling months except for September 2013
507 where the maximum rates were situated between 10-15 cmbsf. In addition to the surface peaks, net
508 methanogenesis showed subsurface (= below 1 cmbsf until 30 cmbsf) maxima at all sampling
509 months, but with alternating depths (between 10 and 25 cmbsf).
510 Comparison of integrated net methanogenesis rates (0-25 cmbsf) revealed highest rates in
511 September and November 2013 (0.09 mmol m⁻² d⁻¹ and 0.08 mmol m⁻² d⁻¹, respectively) and lowest
512 rates in March 2014 (0.01 mmol m⁻² d⁻¹)(Fig. 5). A trend of increasing areal net methanogenesis rates
513 from March to September was observed in both years.

514 **3.4.2 Hydrogenotrophic methanogenesis**

515 Hydrogenotrophic methanogenesis activity determined by ¹⁴C-bicarbonate incubations of MUC cores
516 is shown in Fig. 2 and 3. In 2013, maximum activity ranged between 0.01-0.2 nmol cm⁻³ d⁻¹, while in
517 2014 maxima ranged only between 0.01 and 0.05 nmol cm⁻³ d⁻¹. In comparison, maximum
518 hydrogenotrophic methanogenesis was up to two orders of magnitude lower compared to net
519 methanogenesis. Only in March 2013 both activities reached a similar range.

520 Overall, hydrogenotrophic methanogenesis increased with depth in March, September, and
521 November 2013 and in March, June, and September 2014. In June 2013, activity decreased with
522 depth, showing the highest rates in the upper 0-5 cmbsf and the lowest at the deepest sampled
523 depth.

524 Concomitant with integrated net methanogenesis, integrated hydrogenotrophic methanogenesis
525 rates (0-25 cmbsf) were high in September 2013, with slightly higher rates in March 2013 (Fig. 5).

526 Lowest areal rates of hydrogenotrophic methanogenesis were seen in June of both years.

527 Hydrogenotrophic methanogenesis activity in the gravity core is shown in Fig. 4. Highest activity (~
528 0.7 nmol cm⁻³ d⁻¹) was measured at 45 cmbsf and 138 cmbsf, followed by a decrease with increasing
529 sediment depth reaching 0.01 nmol cm⁻³ d⁻¹ at the deepest sampled depth (345 cmbsf).

530 **3.4.3 Potential methanogenesis in manipulated experiments**

531 Potential methanogenesis rates in manipulated experiments included either the addition of
532 inhibitors (molybdate for inhibition of sulfate reduction or BES for inhibition of methanogenesis) or
533 the addition of a non-competitive substrate (methanol). Control treatments were run with neither
534 the addition of inhibitors nor the addition of methanol.

535 *Controls.* Potential methanogenesis activity in the control treatments was below 0.5 nmol cm⁻³ d⁻¹
536 from March 2014 to September 2014 (Fig. 6). Only in November 2013, control rates exceeded 0.5

537 $\text{nmol cm}^{-3} \text{d}^{-1}$ below 6 cmbsf. While rates increased with depth in November 2013 and June 2014,
538 they decreased with depth at the other two sampling months.

539 *Molybdate*. Peak potential methanogenesis rates in the molybdate treatments were found in the
540 uppermost sediment interval (0-1 cmbsf) at almost every sampling month with rates being 3-30
541 times higher compared to the control treatments ($< 0.5 \text{ nmol cm}^{-3} \text{d}^{-1}$). In November 2013, potential
542 methanogenesis showed two maxima (0-1 and 10-15 cmbsf). Highest measured rates were found in
543 September 2014 ($\sim 6 \text{ nmol cm}^{-3} \text{d}^{-1}$), followed by November 2013 ($\sim 5 \text{ nmol cm}^{-3} \text{d}^{-1}$).

544 *BES*. Profiles of potential methanogenesis in the BES treatments were similar to the controls mostly
545 in the lower range $< 0.5 \text{ nmol cm}^{-3} \text{d}^{-1}$. Only in November 2013 rates exceeded $0.5 \text{ nmol cm}^{-3} \text{d}^{-1}$.
546 Rates increased with depth at all sampling months, except for September 2014, where highest rates
547 were found at the sediment surface (0-1 cmbsf).

548 *Methanol*. At all sampling months, potential rates in the methanol treatments were three orders of
549 magnitude higher compared to the control treatments ($< 0.5 \text{ nmol cm}^{-3} \text{d}^{-1}$). Except for November
550 2013, potential methanogenesis rates in the methanol treatments were highest in the upper 0-5
551 cmbsf and decreased with depth. In November 2013, highest rates were detected at the deepest
552 sampled depth (20-25 cmbsf).

553

554 **3.4.4 Potential methanogenesis followed by ^{13}C -methanol labeling**

555 The concentration of total methanol concentrations (labeled and unlabeled) in the sediment
556 decreased sharply in the first 2 weeks from $\sim 8 \text{ mM}$ at day 1 to 0.5 mM at day 13 (Fig. 7). At day 17,
557 methanol was below the detection limit. In the first 2 weeks, residual methanol was enriched with
558 ^{13}C , reaching $\sim 200 \text{ ‰}$ at day 13.

559 Over the same time period, the methane content in the headspace increased from 2 ppmv at day 1
560 to $\sim 66,000 \text{ ppmv}$ at day 17 and stayed around that value until the end of the total incubation time
561 (until day 37) (Fig. 7). The carbon isotopic signature of methane ($\delta^{13}\text{C}_{\text{CH}_4}$) showed a clear enrichment
562 of the heavier isotope ^{13}C (Table 3) from day 9 to 17 (no methane was detectable at day 1). After day
563 17, $\delta^{13}\text{C}_{\text{CH}_4}$ stayed around 13 ‰ until the end of the incubation. The content of CO_2 in the headspace
564 increased from $\sim 8900 \text{ ppmv}$ at day 1 to $\sim 29,000 \text{ ppmv}$ at day 20 and stayed around $30,000 \text{ ppmv}$
565 until the end of the incubation (Fig. 7). Please note, that the major part of CO_2 was dissolved in the
566 porewater, thus the CO_2 content in the headspace does not show the total CO_2 abundance in the
567 system. CO_2 in the headspace was enriched with ^{13}C during the first 2 weeks (from -16.2 to -7.3 ‰)
568 but then stayed around -11 ‰ until the end of the incubation.

569 **3.5 Molecular analysis of benthic methanogens**

570 In September 2014, additional samples were run during the methanol treatment (see Sect. 2.7.) for
571 the detection of benthic methanogens via qPCR. The qPCR results are shown in Fig. 8. For a better

572 comparison, the microbial abundances are plotted together with the sediment methane
573 concentrations from the methanol treatment, from which the rate calculation for the methanol-
574 methanogenesis at 0-1 cmbsf was done (shown in Fig. 6).
575 Sediment methane concentrations increased over time revealing a slow increase in the first ~10 days,
576 followed by a steep increase between day 13 and day 20 and ending in a stationary phase.
577 A similar increase was seen in the abundance of total and methanogenic archaea. Total archaea
578 abundances increased sharply in the second week of the incubation reaching a maximum at day 16
579 ($\sim 5000 \cdot 10^6$ copies g^{-1}) and stayed around $3000 \cdot 10^6$ - $4000 \cdot 10^6$ copies g^{-1} over the course of the
580 incubation. Similarly, methanogenic archaea, namely the order *Methanosarcinales* and within this
581 order the family *Methanosarcinaceae*, showed a sharp increase in the first 2 weeks as well with the
582 highest abundances at day 16 ($\sim 6 \cdot 10^8$ copies g^{-1} and $\sim 1 \cdot 10^6$ copies g^{-1} , respectively). Until the end of
583 the incubation, the abundances of *Methanosarcinales* and *Methanosarcinaceae* decreased to about a
584 third of their maximum abundances ($\sim 2 \cdot 10^8$ copies g^{-1} and $\sim 0.4 \cdot 10^6$ copies g^{-1} , respectively).

585 3.6 Statistical Analysis

586 The PCA of integrated SRZ methanogenesis (0-5 cmbsf) (Fig. 10) showed a positive correlation with
587 bottom water temperature (Fig. 10a), bottom water salinity (Fig. 10a), bottom water methane (Fig.
588 10b), surface sediment POC content (0-5 cmbsf, Fig. 10c), and surface sediment C/N (0-5 cmbsf, Fig.
589 10b). A negative correlation was found with bottom water oxygen concentration (Fig. 10b). No
590 correlation was found with bottom water chlorophyll.

591 The PCA of methanogenesis depth profiles showed positive correlations with sediment depth (Fig.
592 11a) and C/N (Fig. 11b), and showed negative correlations with POC (Fig. 11a).

593

594 4. Discussion

595 4.1 Methanogenesis in the sulfate-reducing zone

596 On the basis of the results presented in Fig. 2 and 3, it is evident that methanogenesis and sulfate
597 reduction were concurrently active in the sulfate reduction zone (0-30 cmbsf) at Boknis Eck. Even
598 though sulfate reduction activity was not directly determined, the decrease in sulfate concentrations
599 with a concomitant increase in sulfide within the upper 30 cmbsf clearly indicated its presence (Fig. 2
600 and 3). Several previous studies confirmed the high activity of sulfate reduction in the surface
601 sediment of Eckernförde Bay, revealing rates up to 100 - $10,000$ $nmol\ cm^{-3}\ d^{-1}$ in the upper 25 cmbsf
602 (Treude et al., 2005a; Bertics et al., 2013; Dale et al., 2013). Microbial fermentation of organic matter
603 was probably high in the organic-rich sediments of Eckernförde Bay (POC contents of around 5 %, Fig.
604 2 and 3), providing high substrate availability and variety for methanogenesis.

605
606 The results of this study further identified methylotrophy to be a potentially important non-
607 competitive methanogenic pathway in the sulfate-reducing zone. The pathway utilizes alternative
608 substrates, such as methanol, to bypass competition with sulfate reducers for H₂ and acetate. A
609 potential for methylotrophic methanogenesis within the sulfate-reducing zone was supported by the
610 following observations;

- 611 1) Hydrogenotrophic methanogenesis was up to two orders of magnitude lower compared to
612 net methanogenesis, resulting in insufficient rates to explain the observed net
613 methanogenesis in the upper 0-30 cmbsf (Fig. 2 and 3). This finding points towards the
614 presence of alternative methanogenic processes in the sulfate reduction zone, such as
615 methylotrophic methanogenesis.
- 616 2) Methanogenesis increased when sulfate reduction was inhibited by molybdate, confirming
617 the inhibitory effect of sulfate reduction on methanogenesis with competitive substrates (H₂
618 and acetate (Oremland & Polcin, 1982; King et al., 1983)) (Fig. 6). Consequently, usage of
619 non-competitive substrates was preferred in sulfate reduction zone (especially in the upper
620 0-1 cmbsf, Fig. 6). Accordingly, hydrogenotrophic methanogenesis increased at depths where
621 sulfate was depleted and thus the competitive situation was relieved (Fig. 4).
- 622 3) 3) The addition of BES did not result in the inhibition of methanogenesis, indicating the
623 presence of unconventional methanogenic groups using non-competitive substrates (Fig. 7).
624 The unsuccessful inhibition by BES can be explained either by incomplete inhibition or by the
625 fact that the methanogens were insensitive to BES (Hoehler et al., 1994; Smith & Mah, 1981;
626 Santoro & Konisky, 1987). The BES concentration applied in the present study (60 mM) has
627 been shown to result in successful inhibition of methanogens in previous studies (Hoehler et
628 al., 1994). Therefore, the presence of methanogens that are insensitive to BES is more likely.
629 The insensitivity to BES in methanogens is explained by heritable changes in BES permeability
630 or formation of BES-resistant enzymes (Smith & Mah, 1981; Santoro & Konisky, 1987). Such
631 BES resistance was found in *Methanosarcina* mutants (Smith & Mah, 1981; Santoro &
632 Konisky, 1987). This genus was successfully detected in our samples (for more details see
633 point 5), and is known for mediating the methylotrophic pathway (Keltjens & Vogels, 1993),
634 supporting our hypothesis on the utilization of non-competitive substrates by methanogens.
- 635 4) The addition of methanol to sulfate-rich sediments increased methanogenesis rates up to
636 three orders of magnitude, confirming the potential of the methanogenic community to
637 utilize non-competitive substrates especially in the 0-5 cmbsf sediment horizon (Fig. 6). At
638 this sediment depth either the availability of non-competitive substrates, including
639 methanol, was highest (derived from fresh organic matter), or the usage of non-competitive

640 substrates was increased due to the high competitive situation as sulfate reduction is most
641 active in the 0-5 cmbsf layer (Treude et al., 2005a; Bertics et al., 2013). It should be noted
642 that even though methanogenesis rates were calculated assuming a linear increase in
643 methane concentration over the entire incubation to make a better comparison between
644 different treatments, the methanol treatments generally showed a delayed response in
645 methane development (Fig. 8, Supplement, Fig. S2). We suggest that this delayed response
646 was a reflection of cell growth by methanogens utilizing the surplus methanol. We are
647 therefore unable to decipher whether methanol plays a major role as a substrate in the
648 Eckernförde Bay sediments compared to possible alternatives, as its concentration is
649 relatively low in the natural setting (~1 μ M between 0 and 25 cmbsf, June 2014 sampling, G.-
650 C. Zhuang unpubl. data). It is conceivable that other non-competitive substrates, such as
651 methylated sulfides (e.g., dimethyl sulfide or methanethiol), are more relevant for the
652 support of SRZ methanogenesis.

653 5) Methylophilic methanogens of the order *Methanosarcinales* were detected in the
654 methanol-treatment (Fig. 8), confirming the presence of methanogens that utilize non-
655 competitive substrates in the natural environment (Boone et al., 1993), (Fig. 8). The delay in
656 growth of *Methanosarcinales* moreover hints towards the predominant usage of other non-
657 competitive substrates over methanol (see also point 4).

658 6) Stable isotope probing revealed highly ^{13}C -enriched methane produced from ^{13}C -labelled
659 methanol, furthermore confirming the potential of the methanogenic community to utilize
660 non-competitive substrates (Fig. 7). The production of both methane and CO_2 from methanol
661 has been shown previously in different strains of methylophilic methanogens (Penger et al.,
662 2012). The fast conversion of methanol to methane and CO_2 (methanol was consumed
663 completely in 17 days) is hinting towards the presence of methylophilic methanogens (e.g.
664 members of the family *Methanosarcinaceae*, which is known for the methylophilic pathway
665 (Keltjens & Vogels, 1993)). Please note, however, that the storage of the cores (3.5 months)
666 prior to sampling could have led to shifts in the microbial community and thus might not
667 reflect in-situ conditions of the original microbial community in September 2014. The delay in
668 methane production also seen in the stable isotope experiment was, however, only slightly
669 different (methane developed earlier, between day 8 and 12, data not shown) from the non-
670 labeled methanol treatment (between day 10 to 16, Fig. S2), which leads us to the
671 assumption that the storage time at 1°C did not dramatically affect the methanogen
672 community. Similar, in a previous study with arctic sediments, addition of substrates had no
673 stimulatory effect on the rate of methanogenesis or on the methanogen community
674 structure at low temperatures (5°C, (Blake et al., 2015)).

675 **4.2 Environmental control of methanogenesis in the sulfate reduction zone**

676 SRZ methanogenesis in Eckernförde Bay sediments showed variations throughout the sampling
677 period, which may be influenced by variable environmental factors such as temperature, salinity,
678 oxygen, and organic carbon. In the following, we will discuss the potential impact of those factors on
679 the magnitude and distribution of SRZ methanogenesis.

680 **4.2.1 Temperature**

681 During the sampling period, bottom water temperatures increased over the course of the year from
682 late winter (March, 3-4 °C) to autumn (November, 12°C, Fig. 2 and 3). The PCA revealed a positive
683 correlation between bottom water temperature and integrated SRZ methanogenesis (0-5 cmbsf). A
684 temperature experiment conducted with sediment from ~75 cmbsf in September 2014 within a
685 parallel study revealed a mesophilic temperature optimum of methanogenesis (20 °C, data not
686 shown). Whether methanogenesis in the sulfate reduction zone (0-30 cm) has the same physiology
687 remains speculative. However, AOM organisms, which are closely related to methanogens (Knittel &
688 Boetius, 2009), studied in the sulfate reduction zone from the same site were confirmed to have a
689 mesophilic physiology, too (Treude et al. 2005). The sum of these aspects lead us to the conceivable
690 conclusion that SRZ methanogenesis activity in the Eckernförde Bay is positively impacted by
691 temperature increases. Such a correlation between benthic methanogenesis and temperature has
692 been found in several previous studies from different environments ((Sansone & Martens, 1981; Crill
693 & Martens, 1983; Martens & Klump, 1984).

694

695 **4.2.2 Salinity and oxygen**

696 From March 2013 to November 2013, and from March 2014 to September 2014, salinity increased in
697 the bottom-near water (25 m) from 19 to 23 PSU and from 22 to 25 PSU (Fig. 2 and 3), respectively,
698 due the pronounced summer stratification in the water column between saline North Sea water and
699 less saline Baltic Sea water (Bange et al., 2011). The PCA detected a positive correlation between
700 integrated SRZ methanogenesis (0-5 cmbsf) and salinity in the bottom-near water (Fig. 10a). This
701 correlation can hardly be explained by salinity alone, as methanogens feature a broad salinity range
702 from freshwater to hypersaline (Zinder, 1993). More likely, salinity serves as an indicator of water-
703 column stratification, which is often correlated with low O₂ concentrations in the Eckernförde Bay
704 (Fig. S3, Bange et al., 2011; Bertics et al., 2013). Methanogenesis is sensitive to O₂ (Oremland, 1988;
705 Zinder, 1993), and hence conditions might be more favorable during hypoxic or anoxic events,
706 particular in the sediment closest to the sediment-water interface, but potentially also in deeper
707 sediment layers due to the absence of bioturbating and bioirrigating infauna (Dale et al., 2013;
708 Bertics et al., 2013), which could introduce O₂ beyond diffusive transport. Accordingly, the PCA

709 revealed a negative correlation between O₂ concentration close to the seafloor and SRZ
710 methanogenesis.

711

712 **4.2.4 Particulate organic carbon**

713 The supply of particulate organic carbon (POC) is one of the most important factors controlling
714 benthic heterotrophic processes, as it determines substrate availability and variety (Jørgensen,
715 2006). In Eckernförde Bay, the organic material reaching the seafloor originates mainly from
716 phytoplankton blooms in spring, summer and autumn (Bange et al., 2011). It has been estimated that
717 >50 % in spring (February/March), <25 % in summer (July/August) and >75 % in autumn
718 (September/October) of these blooms is reaching the seafloor (Smetacek et al., 1984), resulting in a
719 overall high organic carbon content of the sediment (5 wt %), which leads to high benthic microbial
720 degradation rates including sulfate reduction and methanogenesis (Whiticar, 2002; Treude et al.,
721 2005a; Bertics et al., 2013). Previous studies revealed that high organic matter availability can relieve
722 competition between sulfate reducers and methanogens in sulfate-containing, marine sediments
723 (Oremland et al., 1982; Holmer & Kristensen, 1994; Treude et al., 2009; Maltby et al., 2016).
724 To determine the effect of POC concentration and C/N ratio (the latter as a negative indicator for the
725 freshness of POC) on SRZ methanogenesis, two PCAs were conducted with a) the focus on the upper
726 0-5 cmbsf, which is directly influenced by freshly sedimented organic material from the water column
727 (Fig. 10), and b) the focus on the depth profiles throughout the sediment cores (up to 30 cmbsf) (Fig.
728 11).

729 **a) Effect of POC and C/N ratio in the upper 0-5 cmbsf**

730 For the upper 0-5 cmbsf in the sediment, a positive correlation was found between SRZ
731 methanogenesis (integrated) and POC content (averaged) (Fig. 10c), indicating that POC content is an
732 important controlling factor for methanogenesis in this layer. In support, highest bottom-near water
733 chlorophyll concentrations coincided with highest bottom-near water methane concentrations and
734 high integrated SRZ methanogenesis (0-5 cmbsf) in September 2013, probably as a result of the
735 sedimentation of the summer phytoplankton bloom (Fig. 9). Indeed, the PCA revealed a positive
736 correlation between integrated SRZ methanogenesis rates and bottom-near water methane
737 concentrations (Fig. 10b), when viewed over all investigated months. However, no correlation was
738 found between bottom water chlorophyll and integrated SRZ methanogenesis rates (Fig. 10). As seen
739 in Fig. 9, bottom-near high chlorophyll concentrations did not coincide with high bottom-near
740 methane concentration in June/September 2014. We explain this result by a time lag between
741 primary production in the water column and the export of the produced organic material to the
742 seafloor, which was probably even more delayed during stratification. Such a delay was observed in a
743 previous study (Bange et al., 2010), revealing enhanced water methane concentration close to the

744 seafloor approximately one month after the chlorophyll maximum. The C/N ratio (averaged over 0-5
745 cmbsf) also showed no correlation with integrated methanogenesis from the same depth layer (0-5
746 cmbsf), which is surprising as we expected that a higher C/N ratio, indicative for less labile organic
747 carbon, should have a negative effect on non-competitive methanogenesis. However, methanogens
748 are not able to directly use most of the labile organic matter due their inability to process large
749 molecules (more than two C-C bondings) (Zinder, 1993). Methanogens are dependent on other
750 microbial groups to degrade large organic compounds (e.g. amino acids) for them (Zinder, 1993).
751 Because of this substrate speciation and dependence, a delay between the sedimentation of fresh,
752 labile organic matter and the increase in methanogenesis can be expected, which would not be
753 captured by the applied PCA.

754 *b) Effect of POC and C/N ratio over 0-30 cmbsf*

755 In the PCA for the sediment profiles from the sulfate reduction zone (0-30 cmbsf), POC showed a
756 negative correlation with methanogenesis and sediment depth, while C/N ratio showed a positive
757 correlation with methanogenesis and sediment depth (Fig 11.). Given that POC remained basically
758 unchanged over the top 30 cmbsf, with the exemption of the topmost sediment layer, its negative
759 correlation with methanogenesis is probably solely explained by the increase of methanogenesis
760 with sediment depth, and can therefore be excluded as a major controlling factor. As sulfate in this
761 zone was likely never depleted to levels that are critically limiting sulfate reduction (lowest
762 concentration 1300 μM , compare e.g. with Treude et al., 2014) we do not expect a significant change
763 in the competition between methanogens and sulfate reducers. It is therefore more likely that the
764 progressive degradation of labile POC into dissolvable methanogenic substrates over depth and time
765 had a positive impact on methanogenesis. The C/N ratio indicates such a trend as the labile fraction
766 of POC decreased with depth.

767 **4.3 Relevance of methanogenesis in the sulfate reduction zone of Eckernförde Bay sediments**

768 The time series station Boknis Eck in Eckernförde Bay is known for being a methane source to the
769 atmosphere throughout the year due to supersaturated waters, which result from significant benthic
770 methanogenesis and emission (Bange et al., 2010). The benthic methane formation is thought to take
771 place mainly in sediments below the SMTZ (Treude et al., 2005a; Whiticar, 2002).

772 In the present study, we show that SRZ methanogenesis within the sulfate zone is present despite
773 sulfate concentrations > 1 mM, a limit above which methanogenesis has been thought to be
774 negligible (Alperin et al., 1994; Hoehler et al., 1994; Burdige, 2006), and thus could contribute to
775 benthic methane emissions. In support of this hypothesis, high dissolved methane concentration in
776 the water column occurred with concomitant high SRZ methanogenesis activity (Fig. 9). However,
777 whether the observed water-column methane originated from SRZ methanogenesis or from gas
778 ebullition caused by methanogenesis below the SMTZ, or a mixture of both, remains speculative.

779 How much of the methane produced in the surface sediment is ultimately emitted into the water
780 column depends on the rate of methane consumption, i.e., aerobic and anaerobic oxidation of
781 methane in the sediment (Knittel & Boetius, 2009) (Fig. 1). In organic-rich sediments, such as in the
782 presented study, the oxygenated sediment layer is often only mm-thick, due to the high O₂ demand
783 of microorganisms during organic matter degradation (Jørgensen, 2006; Preisler et al., 2007). Thus,
784 the anaerobic oxidation of methane (AOM) might play a more important role for methane
785 consumption in the studied Eckernförde Bay sediments. In an earlier study from this site, AOM
786 activity was detected throughout the top 0-25 cmbsf, which included zones that were well above the
787 actual SMTZ (Treude et al., 2005a). But the authors concluded that methane oxidation was
788 completely fueled by methanogenesis from below sulfate penetration, as integrated AOM rates (0.8-
789 1.5 mmol m⁻² d⁻¹) were in the same range as the predicted methane flux (0.66-1.88 mmol m⁻² d⁻¹) into
790 the SMTZ.

791 Together with the data set presented here we postulate that AOM above the SMTZ (0.8 mmol m⁻² d⁻¹,
792 Treude et al., (2005a) could be partially or entirely fueled by SRZ methanogenesis. A similar close
793 coupling between methane oxidation and methanogenesis in the absence of definite methane
794 profiles was recently proposed from isotopic labeling experiments with sediments from the sulfate
795 reduction zone of the close-by Aarhus Bay, Denmark (Xiao et al., 2017). It is therefore likely that such
796 a cryptic methane cycling also occurs in the sulfate reduction zone of sediments in the Eckernförde
797 Bay. If, in an extreme scenario, SRZ methanogenesis would represent the only methane source for
798 AOM above the SMTZ, then maximum SRZ methanogenesis could be in the order of 1.6 mmol m⁻² d⁻¹
799 (1.5 mmol m⁻² d⁻¹ AOM + 0.09 mmol m⁻² d⁻¹ net SRZ methanogenesis).

800 Even though the contribution of SRZ methanogenesis to AOM above the SMTZ remains speculative, it
801 leads to the assumption that SRZ methanogenesis could play a much bigger role for benthic carbon
802 cycling in the Eckernförde Bay than previously thought. Whether SRZ methanogenesis at Eckernförde
803 Bay has the potential for the direct emission of methane into the water column goes beyond the
804 scope of this study and should be tested in the future.

805 5. Summary

806 The present study demonstrated that methanogenesis and sulfate reduction were concurrently
807 active within the sulfate-reducing zone in sediments at Boknis Eck (Eckernförde Bay, SW Baltic Sea).
808 The observed methanogenesis was probably based on non-competitive substrates due to the
809 competition with sulfate reducers for the substrates H₂ and acetate. Accordingly, members of the
810 family *Methanosarcinaceae*, which are known for methylotrophic methanogenesis, were found in the
811 sulfate reduction zone of the sediments and are likely to be responsible for the observed
812 methanogenesis with the potential use of non-competitive substrates such as methanol,
813 methylamines or methylated sulfides.

814 Potential environmental factors controlling SRZ methanogenesis are POC content, C/N ratio, oxygen,
815 and temperature, resulting in highest methanogenesis activity during the warm, stratified, and
816 hypoxic months after the late summer phytoplankton blooms.

817 This study provides new insights into the presence and seasonality of SRZ methanogenesis in coastal
818 sediments, and was able to demonstrate that the process could play an important role for the
819 methane budget and carbon cycling of Eckernförde Bay sediments, e.g., by directly fueling AOM
820 above the SMTZ.

821

822 **Author Contribution**

823 J.M. and T.T. designed the experiments. J.M. carried out all experiments. H.W.B. coordinated
824 measurements of water column methane and chlorophyll. C.R.L. and M.A.F. conducted molecular
825 analysis. M.S. coordinated ¹³C-Isotope measurements. J.M. prepared the manuscript with
826 contributions from all co-authors.

827 **Data Availability**

828 Research data for the present study can be accessed via the public data repository PANGAEA
829 (doi:10.1594/PANGAEA.873185).

830 **Acknowledgements**

831 We thank the captain and crew of F.S. Alkor, F.K. Littorina and F.B. Polarfuchs for field assistance. We
832 thank G. Schüssler, F. Wulff, P. Wefers, A. Petersen, M. Lange, and F. Evers for field and laboratory
833 assistance. For the geochemical analysis we want to thank B. Domeyer, A. Bleyer, U. Lomnitz, R.
834 Suhrberg, and V. Thoenissen. We thank F. Malien, X. Ma, A. Kock and T. Baustian for the O₂, CH₄, and
835 chlorophyll measurements from the regular monthly Boknis Eck sampling cruises. Further, we thank
836 R. Conrad and P. Claus at the MPI Marburg for the ¹³C-Methanol measurements. This study received
837 financial support through the Cluster of Excellence "The Future Ocean" funded by the German
838 Research Foundation, through the Sonderforschungsbereich (SFB) 754, and through a D-A-CH project
839 funded by the Swiss National Science Foundation and German Research foundation (grant no.
840 200021L_138057, 200020_159878/1). Further support was provided through the EU COST Action
841 PERGAMON (ESSEM 0902), through the BMBF project BioPara (grant no. 03SF0421B) and through
842 the EU's H2020 program (Marie Curie grant NITROX # 704272 to CRL).

843

844

845

846 **References**

- 847 Abegg, F. & Anderson, A.L. (1997). The acoustic turbid layer in muddy sediments of Eckernförde Bay
848 , Western Baltic : methane concentration , saturation and bubble characteristics. *Marine*
849 *Geology*. 137. pp. 137–147.
- 850 Alperin, M.J., Albert, D.B. & Martens, C.S. (1994). Seasonal variations in production and consumption
851 rates of dissolved organic carbon in an organic-rich coastal sediment. *Geochimica et*
852 *Cosmochimica Acta*. 58 (22). pp. 4909–4930.
- 853 Bakker, D.E., Bange, H.W., Gruber, N., Johannessen, T., Upstill-Goddard, R.C., Borges, A.V., Delille, B.,
854 Löscher, C.R., Naqvi, S.W.A., Omar, A.M. & Santana-Casiano-J.M. (2014). Air-sea interactions of
855 natural long-lived greenhouse gases (CO₂, N₂O, CH₄) in a changing climate. In: P. S. Liss & M. T.
856 Johnson (eds.). *Ocean-Atmosphere Interactions of Gases and Particles*. Heidelberg: Springer-
857 Verlag, pp. 113–169.
- 858 Balzer, W., Pollehne, F. & Erlenkeuser, H. (1986). Cycling of Organic Carbon in a Marine Coastal
859 System. In: P. G. Sly (ed.). *Sediments and Water Interactions*. New York, NY: Springer New York,
860 pp. 325–330.
- 861 Bange, H.W., Bartell, U.H., Rapsomanikis, S. & Andreae, M.O. (1994). Methane in the Baltic and North
862 Seas and a reassessment of the marine emissions of methane. *Global Biogeochemical Cycles*. 8
863 (4). pp. 465–480.
- 864 Bange, H.W., Bergmann, K., Hansen, H.P., Kock, A., Koppe, R., Malien, F. & Ostrau, C. (2010).
865 Dissolved methane during hypoxic events at the Boknis Eck time series station (Eckernförde
866 Bay , SW Baltic Sea). *Biogeosciences*. 7. pp. 1279–1284.
- 867 Bange, H.W., Hansen, H.P., Malien, F., Laß, K., Karstensen, J., Petereit, C., Friedrichs, G. & Dale, A.
868 (2011). Boknis Eck Time Series Station (SW Baltic Sea): Measurements from 1957 to 2010.
869 *LOICZ-Affiliated Activities*. Inprint 20. pp. 16–22.
- 870 Bertics, V.J., Löscher, C.R., Salonen, I., Dale, A.W., Gier, J., Schmitz, R.A. & Treude, T. (2013).
871 Occurrence of benthic microbial nitrogen fixation coupled to sulfate reduction in the seasonally
872 hypoxic Eckernförde Bay, Baltic Sea. *Biogeosciences*. 10 (3). pp. 1243–1258.
- 873 Blake, L.I., Tveit, A., Øvreås, L., Head, I.M. & Gray, N.D. (2015). Response of Methanogens in Arctic
874 Sediments to Temperature and Methanogenic Substrate Availability. *Planet. Space Sci.* 10 (6).
875 pp. 1–18.
- 876 Buckley, D.H., Baumgartner, L.K. & Visscher, P.T. (2008). Vertical distribution of methane metabolism
877 in microbial mats of the Great Sippewissett Salt Marsh. *Environmental microbiology*. 10 (4). pp.
878 967–77.
- 879 Burdige, D.J. (2006). *Geochemistry of Marine Sediments*. New Jersey, U.S.A.: Princeton University
880 Press.
- 881 Cicerone, R.J. & Oremland, R.S. (1988). Biogeochemical aspects of atmospheric methane. *Global*
882 *Biogeochemical Cycles*. 2 (4). pp. 299–327.
- 883 Crill, P. & Martens, C. (1983). Spatial and temporal fluctuations of methane production in anoxic
884 coastal marine sediments. *Limnology and Oceanography*. 28. pp. 1117–1130.
- 885 Crill, P.M. & Martens, C.S. (1986). Methane production from bicarbonate and acetate in an anoxic
886 marine sediment. *Geochimica et Cosmochimica Acta*. 50. pp. 2089–2097.
- 887 Dale, a. W., Bertics, V.J., Treude, T., Sommer, S. & Wallmann, K. (2013). Modeling benthic–pelagic
888 nutrient exchange processes and porewater distributions in a seasonally hypoxic sediment:
889 evidence for massive phosphate release by Beggiatoa? *Biogeosciences*. 10 (2). pp. 629–651.
- 890 Denman, K.L., Brasseur, G., Chidthaisong, A., Ciais, P., Cox, P.M., Dickinson, R.E., Hauglustaine, D.,

- 891 Heinze, C., Holland, E., Jacob, D., Lohmann, U., Ramachandran, S., da Silva Dias, P.L., Wofsy, S.C.
892 & Zhang, X. (2007). Couplings Between Changes in the Climate System and Biogeochemistry. In:
893 S. Solomon, D. Qin, M. Manning, Z. Chen, M. Marquis, K. B. Averyt, M. Tignor, & H. L. Miller
894 (eds.). *Climate Change 2007: The Physical Science Basis. Contribution of Working Group I to the*
895 *Fourth Assessment Report of the Intergovernmental Panel on Climate Change*. Cambridge,
896 United Kingdom and New York, NY, USA: Cambridge University Press.
- 897 EPA (2010). *Methane and nitrous oxide emissions from natural sources*. Washington, DC, USA.
- 898 Ferdelman, T.G., Lee, C., Pantoja, S., Harder, J., Bebout, B.M. & Fossing, H. (1997). Sulfate reduction
899 and methanogenesis in a Thioploca-dominated sediment off the coast of Chile. *Geochimica et*
900 *Cosmochimica Acta*. 61 (15). pp. 3065–3079.
- 901 Gier, J., Sommer, S., Löscher, C.R., Dale, A.W., Schmitz, R.A. & Treude, T. (2016). Nitrogen fixation in
902 sediments along a depth transect through the Peruvian oxygen minimum zone. *Biogeosciences*.
903 13 (14). pp. 4065–4080.
- 904 Grasshoff, K., Ehrhardt, M. & Kremmling, K. (1999). *Methods of Seawater Analysis*. Weinheim: Verlag
905 Chemie.
- 906 Hansen, H.-P., Giesenhausen, H.C. & Behrends, G. (1999). Seasonal and long-term control of bottom-
907 water oxygen deficiency in a stratified shallow-water coastal system. *ICES Journal of Marine*
908 *Science*. 56. pp. 65–71.
- 909 Hartmann, D.L., Klein Tank, A.M.G., Rusticucci, M., Alexander, L.V., Brönnimann, S., Charabi, Y.,
910 Dentener, F.J., Dlugokencky, D.R., Easterling, D.R., Kaplan, A., Soden, B.J., Thorne, P.W., Wild,
911 M. & Zhai, P.M. (2013). Observations: Atmosphere and Surface. In: *Climate Change 2013: The*
912 *Physical Science Basis. Contribution Group I to the Fifth Assessment Report of the*
913 *Intergovernmental Panel on Climate Change*. United Kingdom and New York, NY, USA:
914 Cambridge University Press.
- 915 Hoehler, T.M., Alperin, M.J., Albert, D.B. & Martens, C.S. (1994). Field and laboratory studies of
916 methane oxidation in an anoxic marine sediment: Evidence for a methanogen-sulfate reducer
917 consortium. *Global Biogeochemical Cycles*. 8 (4). pp. 451–463.
- 918 Holmer, M. & Kristensen, E. (1994). Coexistence of sulfate reduction and methane production in an
919 organic-rich sediment. *Marine Ecology Progress Series*. 107. pp. 177–184.
- 920 Jackson, D.R., Williams, K.L., Wever, T.F., Friedrichs, C.T. & Wright, L.D. (1998). Sonar evidence for
921 methane ebullition in Eckernförde Bay. *Continental Shelf Research*. 18. pp. 1893–1915.
- 922 Jørgensen, B.B. (2006). Bacteria and marine Biogeochemistry. In: H. D. Schulz & M. Zabel (eds.).
923 *Marine Geochemistry*. Berlin/Heidelberg: Springer-Verlag, pp. 173–207.
- 924 Jørgensen, B.B. & Parkes, R.J. (2010). Role of sulfate reduction and methane production by organic
925 carbon degradation in eutrophic fjord sediments (Limfjorden, Denmark). *Limnology and*
926 *Oceanography*. 55 (3). pp. 1338–1352.
- 927 Keltjens, J.T. & Vogels, G.D. (1993). Conversion of methanol and methylamines to methane and
928 carbon dioxide. In: J. G. Ferry (ed.). *Methanogenesis: Ecology, Physiology, Biochemistry &*
929 *Genetics*. Chapman & Hall, pp. 253–303.
- 930 King, G.M., Klug, M.J. & Lovley, D.R. (1983). Metabolism of acetate, methanol, and methylated
931 amines in intertidal sediments of lowes cove, maine. *Applied and environmental microbiology*.
932 45 (6). pp. 1848–1853.
- 933 Knittel, K. & Boetius, A. (2009). Anaerobic oxidation of methane: progress with an unknown process.
934 *Annual review of microbiology*. 63. pp. 311–34.
- 935 Lennartz, S.T., Lehmann, A., Herrford, J., Malien, F., Hansen, H.-P., Biester, H. & Bange, H.W. (2014).
936 Long-term trends at the Boknis Eck time series station (Baltic Sea), 1957–2013: does climate
937 change counteract the decline in eutrophication? *Biogeosciences*. 11 (22). pp. 6323–6339.

- 938 Maltby, J., Sommer, S., Dale, A.W. & Treude, T. (2016). Microbial methanogenesis in the sulfate-
 939 reducing zone of surface sediments traversing the Peruvian margin. *Biogeosciences*. 13. pp.
 940 283–299.
- 941 Martens, C.S., Albert, D.B. & Alperin, M.J. (1998). Biogeochemical processes controlling methane in
 942 gassy coastal sediments---Part 1 . A model coupling organic matter flux to gas production ,
 943 oxidation and transport. *Continental Shelf Research*. 18. pp. 14–15.
- 944 Martens, C.S. & Klump, J. V (1984). Biogeochemical cycling in an organic-rich coastal marine basin 4.
 945 An organic carbon budget for sediments dominated by sulfate reduction and methanogenesis.
 946 *Geochimica et Cosmochimica Acta*. 48. pp. 1987–2004.
- 947 Naqvi, S.W. a., Bange, H.W., Farías, L., Monteiro, P.M.S., Scranton, M.I. & Zhang, J. (2010). Marine
 948 hypoxia/anoxia as a source of CH₄ and N₂O. *Biogeosciences*. 7 (7). pp. 2159–2190.
- 949 Oremland, R.S. (1988). Biogeochemistry of methanogenic bacteria. In: A. J. B. Zehnder (ed.). *Biology*
 950 *of Anaerobic Microorganisms*. New York: J. Wiley & Sons, pp. 641–705.
- 951 Oremland, R.S. & Capone, D.G. (1988). Use of specific inhibitors in biogeochemistry and microbial
 952 ecology. In: K. C. Marshall (ed.). *Advances in Microbial Ecology*. Advances in Microbial Ecology.
 953 Boston, MA: Springer US, pp. 285–383.
- 954 Oremland, R.S., Marsh, L.M. & Polcin, S. (1982). Methane production and simultaneous sulfate
 955 reduction in anoxic, salt-marsh sediments. *Nature*. 286. pp. 143–145.
- 956 Oremland, R.S. & Polcin, S. (1982). Methanogenesis and Sulfate Reduction : Competitive and
 957 Noncompetitive Substrates in Estuarine Sediments. *Applied and Environmental Microbiology*. 44
 958 (6). pp. 1270–1276.
- 959 Orsi, T.H., Werner, F., Milkert, D., Anderson, a. L. & Bryant, W.R. (1996). Environmental overview of
 960 Eckernförde Bay, northern Germany. *Geo-Marine Letters*. 16 (3). pp. 140–147.
- 961 Penger, J., Conrad, R. & Blaser, M. (2012). Stable carbon isotope fractionation by methylotrophic
 962 methanogenic archaea. *Applied and environmental microbiology*. 78 (21). pp. 7596–602.
- 963 Pimenov, N., Davidova, I., Belyaev, S., Lein, A. & Ivanov, M. (1993). Microbiological processes in
 964 marine sediments in the Zaire River Delta and the Benguela upwelling region. *Geomicrobiology*
 965 *Journal*. 11 (3–4). pp. 157–174.
- 966 Preisler, A., de Beer, D., Lichtschlag, A., Lavik, G., Boetius, A. & Jørgensen, B.B. (2007). Biological and
 967 chemical sulfide oxidation in a Beggiatoa inhabited marine sediment. *The ISME journal*. 1 (4).
 968 pp. 341–353.
- 969 Reeburgh, W. (2007). Oceanic methane biogeochemistry. *Chemical Reviews*. pp. 486–513.
- 970 Sansone, F.J. & Martens, C.S. (1981). Methane Production from Acetate and Associated Methane
 971 Fluxes from Anoxic Coastal Sediments. *Science*. 211 (4483). pp. 707–709.
- 972 Santoro, N. & Konisky, J. (1987). Characterization of bromoethanesulfonate-resistant mutants of
 973 *Methanococcus voltae*: Evidence of a coenzyme M transport system. *Journal of Bacteriology*.
 974 169 (2). pp. 660–665.
- 975 Schlüter, M., Sauter, E., Hansen, H.-P. & Suess, E. (2000). Seasonal variations of bioirrigation in
 976 coastal sediments: modelling of field data. *Geochimica et Cosmochimica Acta*. 64 (5). pp. 821–
 977 834.
- 978 Seeberg-Elverfeldt, J., Schlüter, M., Feseker, T. & Kolling, M. (2005). Rhizon sampling of porewaters
 979 near the sediment-water interface of aquatic systems. *Limnology and Oceanography-Methods*.
 980 3. pp. 361–371.
- 981 Smetacek, V. (1985). The Annual Cycle of Kiel Bight Plankton: A Long-Term Analysis. *Estuaries*. 8
 982 (June). pp. 145–157.
- 983 Smetacek, V., von Bodungen, B., Knoppers, B., Peinert, R., Pollehne, F., Stegmann, P. & Zeitzschel, B.

- 984 (1984). Seasonal stages characterizing the annual cycle of an inshore pelagic system. *Rapports*
985 *et Proces-Verbaux des Reunions Conseil International pour l'Exploration de la Mer*. 186. pp.
986 126–135.
- 987 Smith, M.R. & Mah, R. a. (1981). 2-Bromoethanesulfonate: A selective agent for isolating
988 resistant *Methanosarcina* mutants. *Current Microbiology*. 6 (5). pp. 321–326.
- 989 Steinle, L., Maltby, J., Treude, T., Kock, A., Bange, H.W., Engbersen, N., Zopfi, J., Lehmann, M.F. &
990 Niemann, H. (2017). Effects of low oxygen concentrations on aerobic methane oxidation in
991 seasonally hypoxic coastal waters. *Biogeosciences*. 14 (6). pp. 1631–1645.
- 992 Thießen, O., Schmidt, M., Theilen, F., Schmitt, M. & Klein, G. (2006). Methane formation and
993 distribution of acoustic turbidity in organic-rich surface sediments in the Arkona Basin, Baltic
994 Sea. *Continental Shelf Research*. 26 (19). pp. 2469–2483.
- 995 Treude, T., Krause, S., Maltby, J., Dale, A.W., Coffin, R. & Hamdan, L.J. (2014). Sulfate reduction and
996 methane oxidation activity below the sulfate-methane transition zone in Alaskan Beaufort Sea
997 continental margin sediments: Implications for deep sulfur cycling. *Geochimica et*
998 *Cosmochimica Acta*. 144. pp. 217–237.
- 999 Treude, T., Krüger, M., Boetius, A. & Jørgensen, B.B. (2005a). Environmental control on anaerobic
1000 oxidation of methane in the gassy sediments of Eckernförde Bay (German Baltic). *Limnology*
1001 *and Oceanography*. 50 (6). pp. 1771–1786.
- 1002 Treude, T., Niggemann, J., Kallmeyer, J., Wintersteller, P., Schubert, C.J., Boetius, A. & Jørgensen, B.B.
1003 (2005b). Anaerobic oxidation of methane and sulfate reduction along the Chilean continental
1004 margin. *Geochimica et Cosmochimica Acta*. 69 (11). pp. 2767–2779.
- 1005 Treude, T., Smith, C.R., Wenzhöfer, F., Carney, E., Bernardino, A.F., Hannides, A.K., Krgüer, M. &
1006 Boetius, A. (2009). Biogeochemistry of a deep-sea whale fall: Sulfate reduction, sulfide efflux
1007 and methanogenesis. *Marine Ecology Progress Series*. 382. pp. 1–21.
- 1008 Welschmeyer, N.A. (1994). Fluorometric analysis of chlorophyll a in the presence of chlorophyll b and
1009 pheopigments. *Limnology and Oceanography*. 39 (8). pp. 1985–1992.
- 1010 Wever, T.F., Abegg, F., Fiedler, H.M., Fechner, G. & Stender, I.H. (1998). Shallow gas in the muddy
1011 sediments of Eckernförde Bay, Germany. *Continental Shelf Research*. 18. pp. 1715–1739.
- 1012 Wever, T.F. & Fiedler, H.M. (1995). Variability of acoustic turbidity in Eckernförde Bay (southwest
1013 Baltic Sea) related to the annual temperature cycle. *Marine Geology*. 125. pp. 21–27.
- 1014 Whitticar, M.J. (2002). Diagenetic relationships of methanogenesis, nutrients, acoustic turbidity,
1015 pockmarks and freshwater seepages in Eckernförde Bay. *Marine Geology*. 182. pp. 29–53.
- 1016 Widdel, F. & Bak, F. (1992). Gram-Negative Mesophilic Sulfate-Reducing Bacteria. In: A. Balows, H. G.
1017 Trüper, M. Dworkin, W. Harder, & K.-H. Schleifer (eds.). *The Prokaryotes*. New York, NY:
1018 Springer New York, pp. 3352–3378.
- 1019 Wuebbles, D.J. & Hayhoe, K. (2002). Atmospheric methane and global change. *Earth-Science Reviews*.
1020 57 (3–4). pp. 177–210.
- 1021 Xiao, K.Q., Beulig, F., Kjeldsen, K.U., Jørgensen, B.B. & Risgaard-Petersen, N. (2017). Concurrent
1022 methane production and oxidation in surface sediment from Aarhus Bay, Denmark. *Frontiers in*
1023 *Microbiology*. pp. 1–12.
- 1024 Zinder, S.H. (1993). Physiological ecology of methanogens. In: J. G. Ferry (ed.). *Methanogenesis*. New
1025 York, NY: Chapman & Hall, pp. 128–206.

1026

1027 **Figure Captions**

1028 **Figure 1:** Overview of processes relevant for benthic methane production, consumption, and
1029 emission in the Eckernförde Bay. The thickness of arrows for emissions and coupling between surface
1030 processes indicates the strength of methane supply. Note that this figure combines existing
1031 knowledge with results from the present study. See discussion for more details.

1032 **Figure 2:** Parameters measured in the water column and sediment in the Eckernförde Bay at each
1033 sampling month in the year 2013. Net methanogenesis (MG) and hydrogenotrophic (hydr.)
1034 methanogenesis rates are shown in triplicates with mean (solid line).

1035 **Figure 3:** Parameters measured in the water column and sediment in the Eckernförde Bay at each
1036 sampling month in the year 2014. Net methanogenesis (MG) and hydrogenotrophic (hydr.)
1037 methanogenesis rates are shown in triplicates with mean (solid line).

1038 **Figure 4:** Parameters measured in the sediment gravity core taken in the Eckernförde Bay in
1039 September 2013. Hydrogenotrophic (hydr.) methanogenesis rates are shown in triplicates with mean
1040 (solid line).

1041 **Figure 5:** Integrated net methanogenesis (MG) rates (determined by net methane production) and
1042 hydrogenotrophic MG rates (determined by radiotracer incubation) in surface sediments (0-25
1043 cmbsf) of Eckernförde Bay for different sampled time points.

1044 **Figure 6:** Potential methanogenesis rates versus sediment depth in sediment sampled in November
1045 2013, March 2014, June 2014 and September 2014. Presented are four different types of incubations
1046 (treatments): *Control* (blue symbols) is describing the treatment with sediment plus artificial
1047 seawater containing natural salinity (24 PSU) and sulfate concentrations (17 mM), *molybdate* (green
1048 symbols) is the treatment with addition of molybdate (22 mM), *BES* (purple symbols) is the
1049 treatment with 60 mM BES addition, and *methanol* (red symbols) is the treatment with addition of 10
1050 mM methanol. Shown are triplicates per depth interval and the mean as a solid line. Please note the
1051 different x-axis for the methanol treatment (red).

1052 **Figure 7:** Development of headspace gas content and isotope composition of methane (CH₄) and
1053 carbon dioxide (CO₂), and porewater methanol (CH₃OH) concentration and isotope composition
1054 during the ¹³C-labeling experiment (with sediment from the 0-2 cmbsf horizon in September 2014)
1055 with addition of ¹³C-enriched methanol (¹³C:¹²C = 1:1000). *Figure above:* Concentrations of porewater
1056 methanol (CH₃OH) and headspace content of methane (CH₄) and carbon dioxide (CO₂) over time.
1057 *Figure below:* Isotope composition of porewater CH₃OH, headspace CH₄, and headspace CO₂ over
1058 time. Shown are means (from triplicates) with standard deviation.

1059 **Figure 8:** Sediment methane concentrations (with sediment from the 0-1 cmbsf in September 2014)
1060 over time in the treatment with addition of methanol (10 mM) are shown above. Shown are triplicate
1061 values per measurement. DNA copies of *Archaea*, *Methanosarcinales* and *Methanosarcinaceae* are
1062 shown below in duplicates per measurement. Please note the secondary y-axis for
1063 *Methanosarcinales* and *Methanosarcinaceae*. More data are available for methane (determined in
1064 the gas headspace) than from DNA samples (taken from the sediment) as sample volume for
1065 molecular analyzes was limited.

1066 **Figure 9:** Temporal development of integrated net surface methanogenesis (0-5 cmbsf) in the
1067 sediment and chlorophyll (green) and methane concentrations (orange) in the bottom water (25 m).
1068 Methanogenesis (MG) rates and methane concentrations are shown in means (from triplicates) with
1069 standard deviation.

1070 **Figure 10:** Principle component analysis (PCA) from three different angles of integrated surface
1071 methanogenesis (0-5 cmbsf) and surface particulate organic carbon averaged over 0-5 cmbsf (surface
1072 sediment POC), surface C/N ratio averaged over 0-5 cmbsf (surface sediment C/N), bottom water
1073 salinity, bottom water temperature (T), bottom water methane (CH₄), bottom water oxygen (O₂), and
1074 bottom water chlorophyll. Data were transformed into ranks before analysis. a) Correlation biplot of
1075 principle components 1 and 2, b) correlation biplot of principle components 1 and 3, c) correlation
1076 biplot of principle components 2 and 3. Correlation biplots are shown in a multidimensional space
1077 with parameters shown as green lines and samples shown as black dots. Parameters pointing into
1078 the same direction are positively related; parameters pointing in the opposite direction are
1079 negatively related.

1080
1081 **Figure 11:** Principle component analysis (PCA) from two different angles of net methanogenesis
1082 depth profiles and sampling month (Month), sediment depth, depth profiles of particulate organic
1083 carbon (POC) and C/N ratio (C/N). Data was transformed into ranks before analysis. a) Correlation
1084 biplot of principle components 1 and 2, b) correlation biplot of principle components 1 and 3.
1085 Correlation biplots are shown in a multidimensional space with parameters shown as green lines and
1086 samples shown as black dots. Parameters pointing into the same direction are positively related;
1087 parameters pointing in the opposite direction are negatively related.

1088

1089

1090

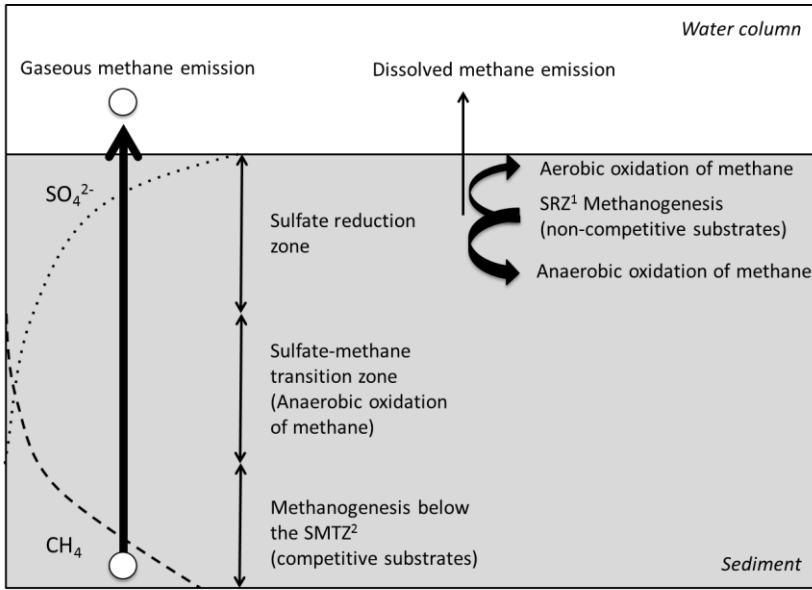
1091 **Table 1:** Sampling months with bottom water (~ 2 m above seafloor) temperature (Temp.), dissolved
 1092 oxygen (O₂) and dissolved methane (CH₄) concentration

Sampling Month	Date	Instrument	Temp. (°C)	O ₂ (µM)	CH ₄ (nM)	Type of Analysis
March 2013	13.03.2013	CTD	3	340	30	WC
		MUC				All
Juni 2013	27.06.2013	CTD	6	94	125	WC
		MUC				All
September 2013	25.09.2013	CTD	10	bdl	262*	WC
		MUC				All
		GC				GC-All
November 2013	08.11.2013	CTD	12	163	13	WC
		MUC				All
March 2014	13.03.2014	CTD	4	209	41*	WC
		MUC				All
June 2014	08.06.2014	CTD	7	47	61	WC
		MUC				All
September 2014	17.09.2014	CTD	13	bdl	234	WC
		MUC				All

1093 MUC = multicorer, GC= gravity corer, CTD = CTD/Rosette, bdl= below detection limit (5µM), All = methane gas
 1094 analysis, porewater analysis, sediment geochemistry, net methanogenesis analysis, hydrogenotrophic
 1095 methanogenesis analysis, GC-All= analysis for gravity cores including methane gas analysis, porewater analysis,
 1096 sediment geochemistry, hydrogenotrophic methanogenesis analysis, WC= Water column analyses including
 1097 methane analysis, chlorophyll analysis
 1098 **Concentrations from the regular monthly Boknis Eck sampling cruises on 24.09.13 and 05.03. 14 (www.bokniseck.de)
 1099
 1100
 1101
 1102
 1103
 1104
 1105
 1106

1107 Figures

1108 Figure 1



¹ SRZ= sulfate reduction zone

² SMTZ= Sulfate-methane-transition-zone

1109

1110

1111

1112

1113

1114

1115

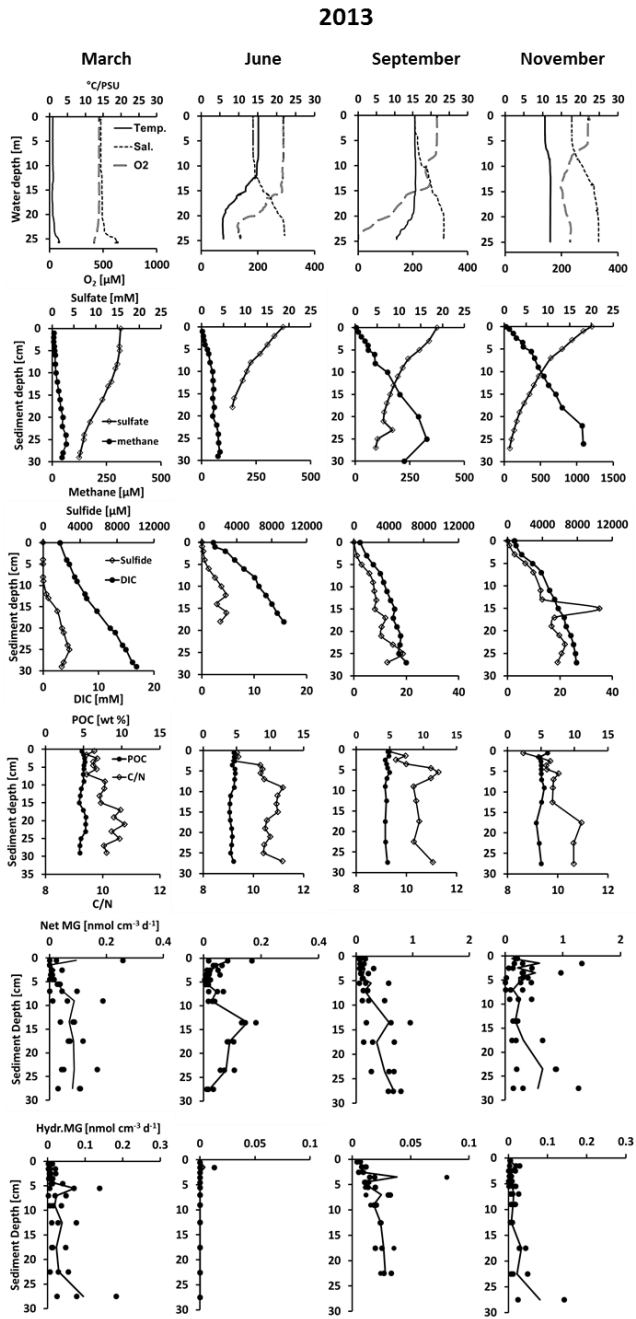
1116

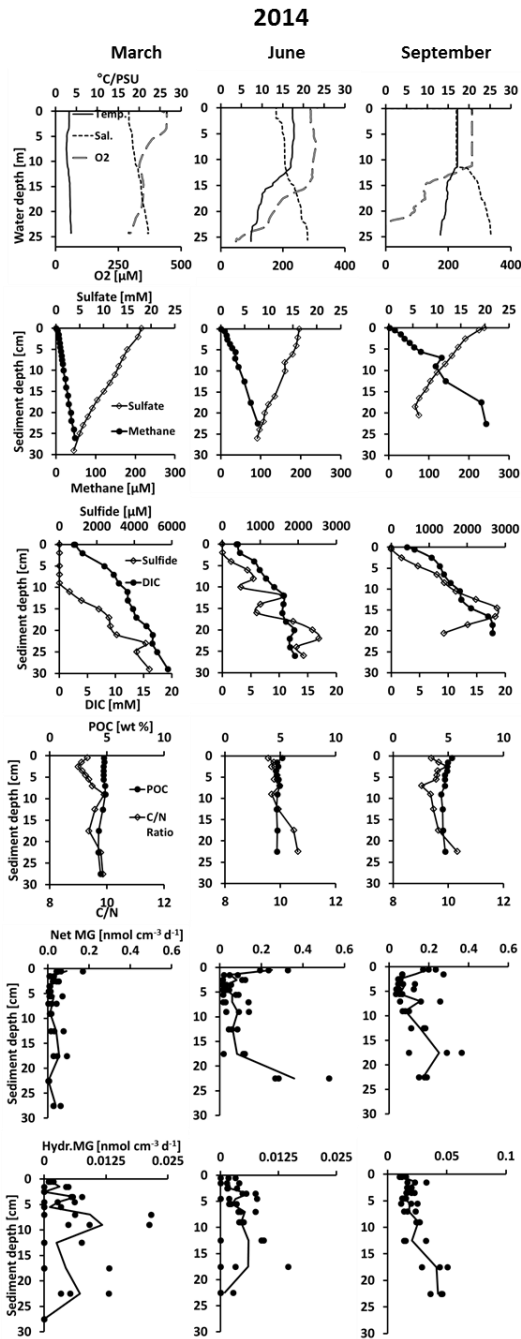
1117

1118

1119

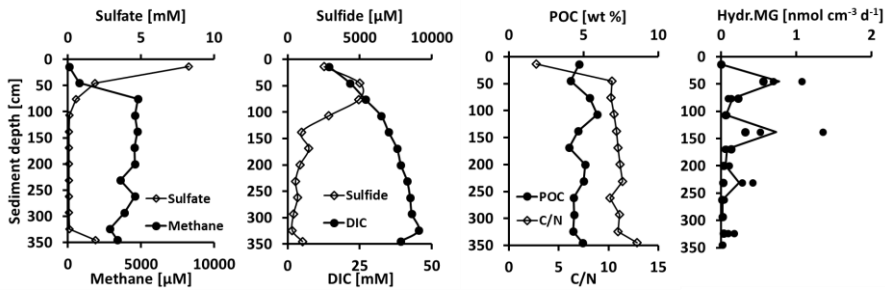
1120





1125 **Figure 4**

1126



1127

1128

1129

1130

1131

1132

1133

1134

1135

1136

1137

1138

1139

1140

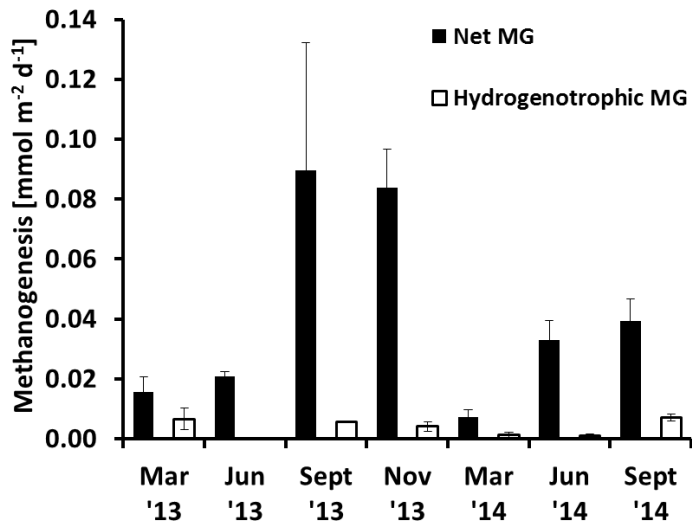
1141

1142

1143

1144 Figure 5

1145



1146

1147

1148

1149

1150

1151

1152

1153

1154

1155

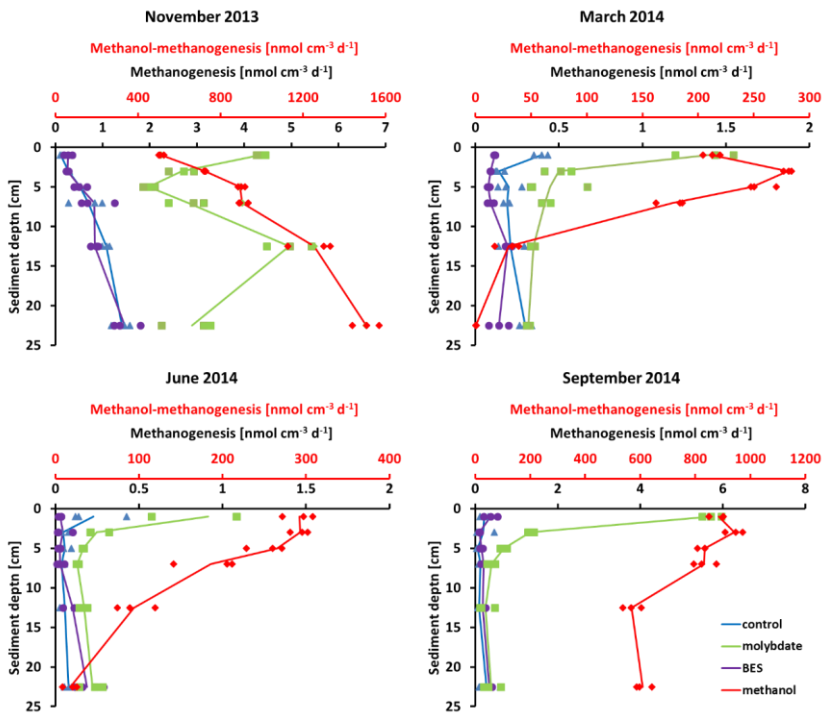
1156

1157

1158

1159 **Figure 6**

1160



1161

1162

1163

1164

1165

1166

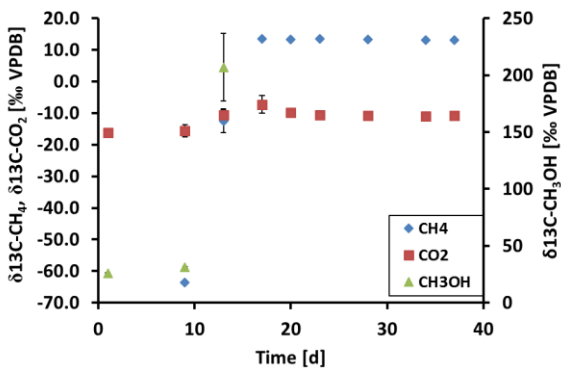
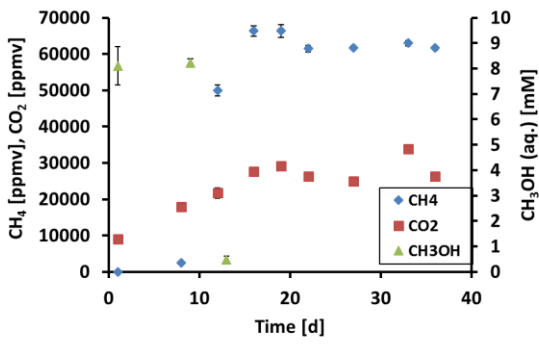
1167

1168

1169

1170

1171 Figure 7



1172

1173

1174

1175

1176

1177

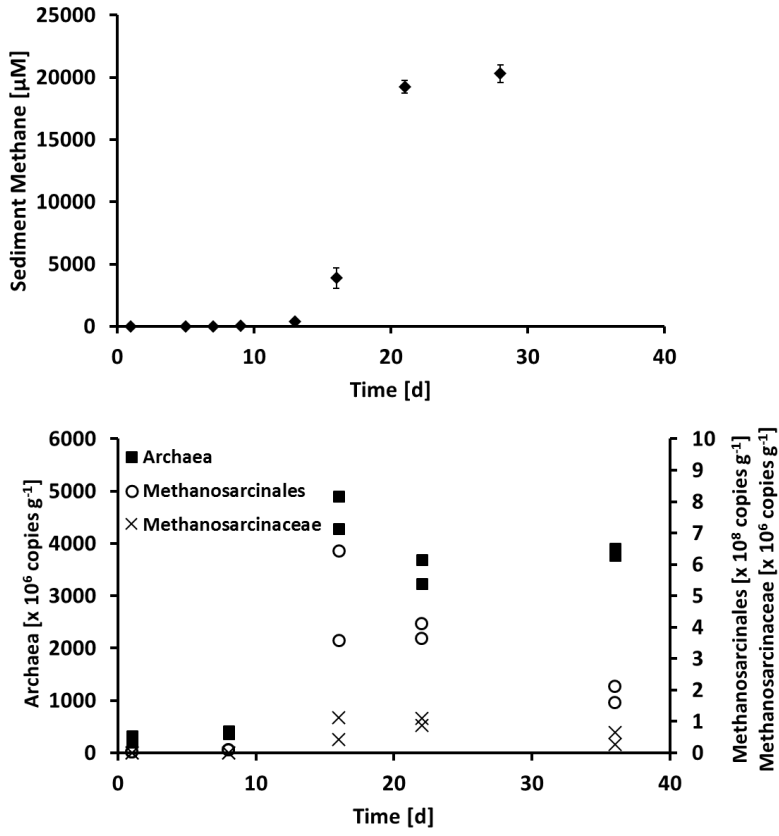
1178

1179

1180

1181

1182 Figure 8



1183

1184

1185

1186

1187

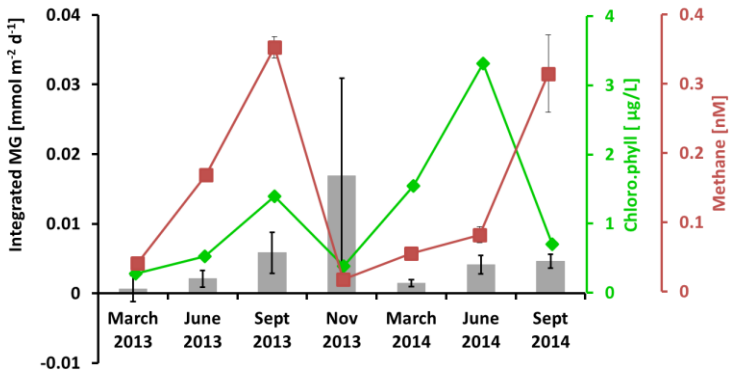
1188

1189

1190

1191

1192 **Figure 9**



1193

1194

1195

1196

1197

1198

1199

1200

1201

1202

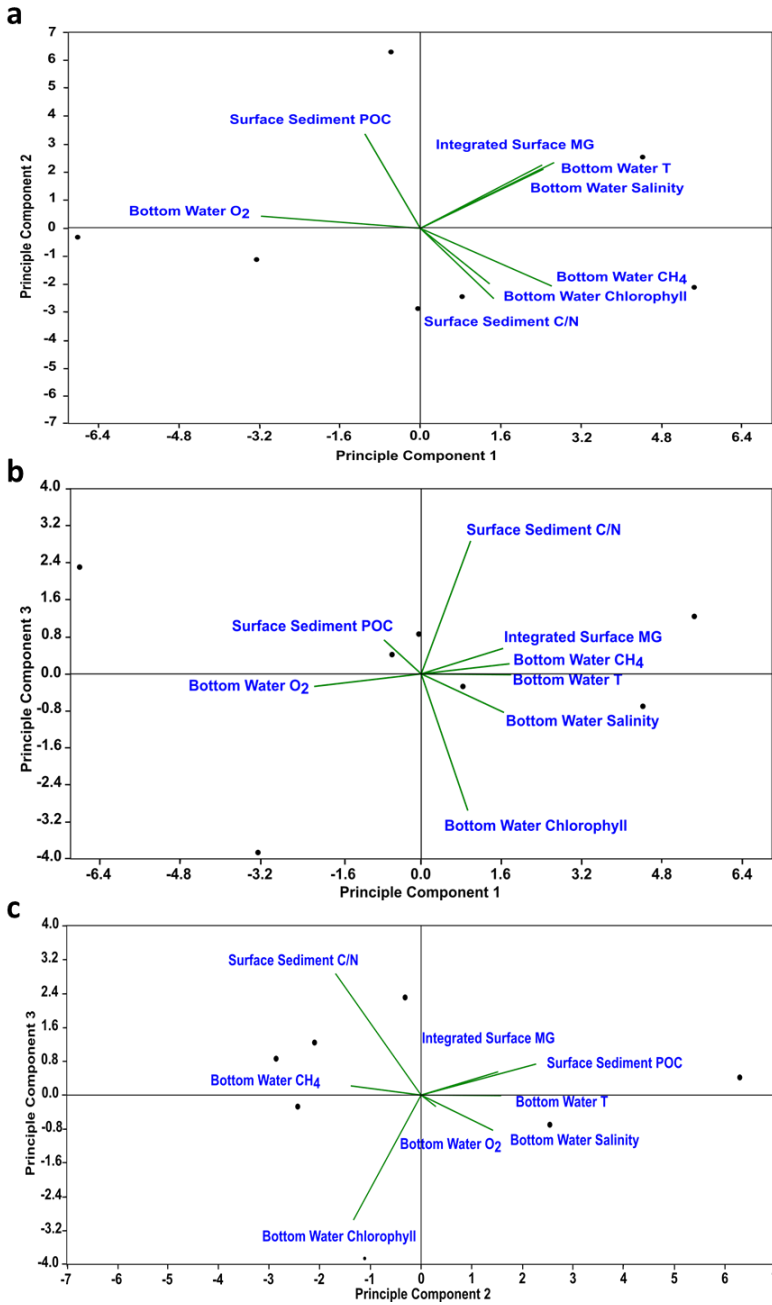
1203

1204

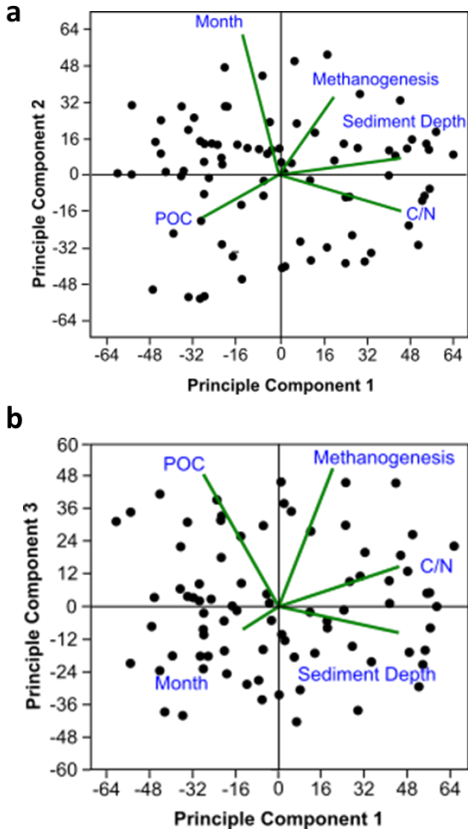
1205

1206

1207



1210 **Figure 11**



1211

1212

1213

1214

1215

1216

1217

1218